

4

NOT FILE COPY

USAFA-TR-89-6



AD-A213 817

**TWO DIMENSIONAL LAMINATED SHELL THEORY INCLUDING
PARABOLIC TRANSVERSE SHEAR**

Captain Scott T. Dennis
Department of Engineering Mechanics
HQ USAFA/DFEM
United States Air Force Academy
Colorado, 80840

October 1989

CS

Approved for public release; distribution unlimited

89 10 27 086


Technical Review by Dr. Stan Jones
Department of Engineering Mechanics
USAF Academy, Colorado 80840

Technical Review by Dr. Anthony N. Palazotto
Air Force Institute of Technology
Wright-Patterson Air Force Base, OH 45433

Editorial Review by Lt Col Donald C. Anderson
Department of English
USAF Academy, Colorado 80840

This research report is presented as a competent treatment of the subject, worthy of publication. The United States Air Force Academy vouches for the quality of the research, without necessarily endorsing the opinions and conclusions of the author.

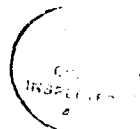
This report has been cleared for open publication and public release by the appropriate Office of Information in accordance with AFM 190-1, AFR 12-30, and AFR 80-3. This report may have unlimited distribution to the public at large, or by DDC to the National Technical Information Service.


RICHARD DURHAM, Lt Col, USAF
Director of Research

Two-Dimensional Laminated Shell Theory

Including Parabolic Transverse Shear

Captain Scott T. Dennis
Department of Engineering Mechanics



A-1

A-1

Abstract

The report presents an approach for a general laminated shell geometry describable by orthogonal curvilinear coordinates. The theory includes a through the thickness parabolic distribution of transverse shear stress. Additionally, a simplified approach that allows large displacements and rotations is incorporated. The theory is cast into a displacement based finite element formulation and then specialized to a cylindrical shell geometry. Linear results are compared to exact elasticity solutions of a laminated cylindrical shell in cylindrical bending. The approach predicts displacement and stress for the unidirectional cases very well even for the very thick laminates. Transverse stress for the cross ply cases are not as accurate since equilibrium at the ply interfaces is not enforced, a typical drawback of 2-D theories.

Preface

The approach presented here is that developed by the author and Dr. Anthony Palazotto (AFIT/EMU) as part of the former's PhD program. Although the theory is geometrically nonlinear, strictly linear stress results are presented herein, see [66] for many other linear and nonlinear shell solutions. The following rough the thickness shell comparisons to exact elasticity solutions demonstrate some of the capabilities and limitations of a relatively simple 2-D approach used to describe generally 3-D phenomena. Once the limitations of the approach are better known, the theory can be applied to new situations where elasticity solutions are not possible. Previously, a similar study compared laminated flat plate results to the well known Pagano exact solutions in [66]. Unfortunately, the exact laminated shell solutions were published very late in the author's PhD program and the present study was not done. This technical report therefore fills that void.

Chapters I, II, and III cover the theoretical aspects of the shell approach and numerical solution technique. These chapters are taken directly from Ref. [67] and allow this report to stand on its own.

Table of Contents

	pg
I. Introduction.....	1
II. Theoretical Development.....	7
III. Finite Element Solution.....	26
IV. Laminated Shell in Cylindrical Bending.....	39
V. Conclusions.....	65
Bibliography.....	66
Appendix.....	71

1. Introduction

Love's shell theory [1] is based on the following assumptions: 1) the shell is thin, therefore neglect transverse normal stress and strain; 2) the shell middle surface (mid-surface) deformation is small after deformation, thereby neglecting transverse shear strain. These assumptions lead to a thin shell theory, that can be viewed as an extension to Kirchhoff's plate theory. Both linear and nonlinear representations of Love shell theory can be derived strictly from definitions of surface theory [2,3,4], or from three dimensional elasticity [1]. Dong, Pister, and Taylor [5] use a small displacement Love theory for the bending analysis of thin anisotropic plates and shells. These are specialized to give linear Donnell equations for anisotropic cylindrical shells. Bert [6] formulated a linear laminated shell theory similar to classical laminated Plate Theory. Bogner, Fox, and Schmit [7] developed a linear cylindrical isotropic shell finite element based upon the classical theory for isotropic materials. Similarly, Yang [8] applied the classical theory to shell geometries of constant curvatures. Cheng and Ho [9] present an exact linear theory for orthotropic cylindrical shells based on Love assumptions where the usual eighth order operator is separated into two complex conjugate operators of only fourth order.

Koiter [10] states that any refinements made to the classical theory should also include transverse deformation

effects. As the shell becomes thicker relative to its radii of curvature and in-plane dimensions, or for laminated composite shells, these transverse effects become more pronounced, especially the transverse shearing. The first theories that included the transverse shear deformation relax the assumption on the deformed normals of the shell middle surface. The shell kinematics introduced by Bassett, as discussed in [11], express the shell displacements as an infinite power series in the thickness coordinate. Hildebrand, Reissner, and Thompson [11] introduced truncated Bassett kinematics to analyze the importance of the transverse stresses and strains in thin elastic orthotropic shells. Naghdi [12] applied similar truncated series representations for general thin isotropic elastic shells. Hildebrand, et al, found that the effects of the second order displacement terms and terms in the transverse displacement that give a nonzero transverse normal strain were negligible. Reissner used similar kinematics to analyze plates [13] and then sandwich shells [14]. Mindlin similarly included rotatory inertia terms in the dynamic analysis of plates [15]. The preceding studies have resulted in the so called Reissner-Mindlin (RM) theory. The approach does not satisfy the transverse shear boundary conditions on the top and bottom surfaces of the shell or plate since a constant shear angle through the thickness is assumed, i.e., plane sections remain plane. Because of this, the theories based on these kinematics usually require

shear correction factors for equilibrium considerations.

Yang, Morris, and Stavsky [16] generalized Reissner-Mindlin plate theory to laminated composite plates. Whitney and Pagano [17] were the first to apply it to composite plate analysis. Reddy [18] has applied RM theory to linear anisotropic shell structures of constant principal and twist curvatures. Noor [19] applies RM theory to examine the stability of laminated plates. Thick composite plate closed form solutions are reported by Reddy and Chao [20]. Linear static, stability, and vibration analyses of laminated plates and shells were performed by Noor and Mathers [21]. Two finite element formulations, mixed and displacement, are compared. Ahmad, Irons, and Zienkiewicz [22] introduced a finite element approach with independent transverse displacement and rotational degrees of freedom such that a Reissner-Mindlin shear deformation shell element results. These elements perform admirably for thick situations, but develop shear locking numerical difficulties for thin cases and consequently, reduced elemental integrations [23] or discrete Kirchhoff constraints [24] become necessary.

Levinson [25], Murthy [26], and Reddy [27] have developed plate theories that include cubic terms in the in-plane displacement kinematics. Satisfying zero transverse shear stress on the top and bottom surfaces of the plate results in a parabolic shear strain distribution through the thickness, thus agreeing more closely with

elasticity results. The number of variables in the kinematics is equal to that in the RM theory, but shear correction factors are not required. Reddy and Phan [28,29] analyzed linear laminated anisotropic plates using the parabolic shear theory. The parabolic shear theory is extended to shell geometries in a study of the linear behavior of laminated shells by Reddy and Liu [30]. Bhimaraddi has applied the parabolic shear strain distribution to analyze the linear vibrational behavior of isotropic cylindrical shells [31] and rings and arches in [32]. Additionally, Soldatos applied the parabolic shear theory to examine the stability and vibrations of laminated circular [33] and noncircular [34] cylindrical shells.

Geometrically nonlinear behavior is captured by allowing large displacements and rotations in the shell strain displacement relations. An approach that neglects the nonlinear terms that represent in-plane rotations of the shell is an example of the intermediate nonlinear theories often used in stability analysis [35,36]. Small strain, moderate rotation approaches for anisotropic shells are given by Librescu and Schmidt [37] and Schmidt and Reddy [70]. Successive approximations made to exact shell strain displacement relations where large strains, displacements, and rotations are all initially allowed, are presented for isotropic shells by Sanders [38] and Pietraszkiewicz [71] and anisotropic shells by Librescu [39].

An early work by Schmit and Monforton [40] formulates

an anisotropic cylindrical shell element based upon the classical theory that allows intermediate geometric nonlinearities. Stolarski et al [41] present a simple triangular shell element formulation that includes intermediate nonlinearity. Reddy and Chandrashekara [42] solve both cylindrical and spherical laminated shell cases assuming RM transverse shear and an intermediate nonlinearity. Reddy [43] analyzed the nonlinear transient behavior of composite plates including RM transverse shear. Putchu and Reddy [44] used the parabolic shear theory in formulating a mixed element for nonlinear anisotropic plate analysis. Noor and Peters [45] give the nonlinear response of anisotropic cylindrical panels via a Hu-Washizu mixed shallow shell finite element approach that includes transverse shear deformation together with a Rayleigh-Ritz technique. Merouch [46] and Surana [47,48] develop geometrically nonlinear shell finite element approaches that are shear deformable. Stein [49] uses truncated series expansions of exact nonlinear strains in a shell approach that also includes transverse shear deformation. Geometrically nonlinear quasi-three-dimensional approaches for laminated composite plates and shells have been developed by Palazotto et al [50,51].

Very recent laminated plate and shell review articles are, respectively, due to Noor and Burton [68] and Kapania [69].

The present report presents an approach for laminated

composite shell analysis that combines a parabolic transverse shear distribution with a simplified large displacement and rotational geometric nonlinearity. Solutions to the theory are found via a displacement based finite element approach. Extensive results are given for the linear analysis of a laminated cylindrical shell in cylindrical bending. This simple case is chosen to illustrate the effectiveness of the 2-D approach in describing 3-D response. Once its limitations are known, the approach can then be applied to the majority of situations where elasticity solutions are not possible.

II. Theoretical Development

General

Although shell theory can be based entirely on surface definitions, transverse shear strains and stresses are then not easily included. One way to define strain displacement relations that can easily incorporate three dimensionality (3-D) is to specialize the general 3-D strain displacement relations expressed in arbitrary orthogonal curvilinear coordinates. To this end, consider the infinitesimal line segment, MN , of length ds embedded in a differential volume element in Figure 1. This differential volume is linearly transformed, i.e., deformed, to a new configuration where the line segment is now of length ds^* . As a result of deformation, the line segment MN of Figure 1 moves to M^*N^* represented by the displacement vector, \underline{u} . By subtracting the original and deformed squared lengths of the line segment, the Green's strain tensor, γ_{ij} ($i, j=1, 2, 3$), is defined as shown in Eqn (1).

$$(ds^*)^2 - (ds)^2 = 2\gamma_{ij} dy_i dy_j \quad (\text{repeated indices sum}) \quad (1)$$

where the y_i are the orthogonal curvilinear coordinates of the undeformed system. The physical strains, ϵ_{ij} , are then found from,

$$\epsilon_{ij} = \frac{\gamma_{ij}}{h_i h_j} \quad (\text{no sum}) \quad (2)$$

In Eqn (2), the h_i are scale factors defined from the

metric tensor of the undeformed coordinate system and the γ_{ij} are shown in the Appendix, Eqn (A1), where the u_i are the coordinates of the displacement vector, \underline{u} . For the case of small strains ($\epsilon < .04$), the ϵ_{ii} (no sum) are the elongations of the fibers of the differential volume element and the ϵ_{ij} ($i \neq j$) are the shears, i.e., the difference from ninety degrees originally perpendicular fibers are oriented after deformation. The elongations and shears are identically zero for rigid body movements of the element [52].

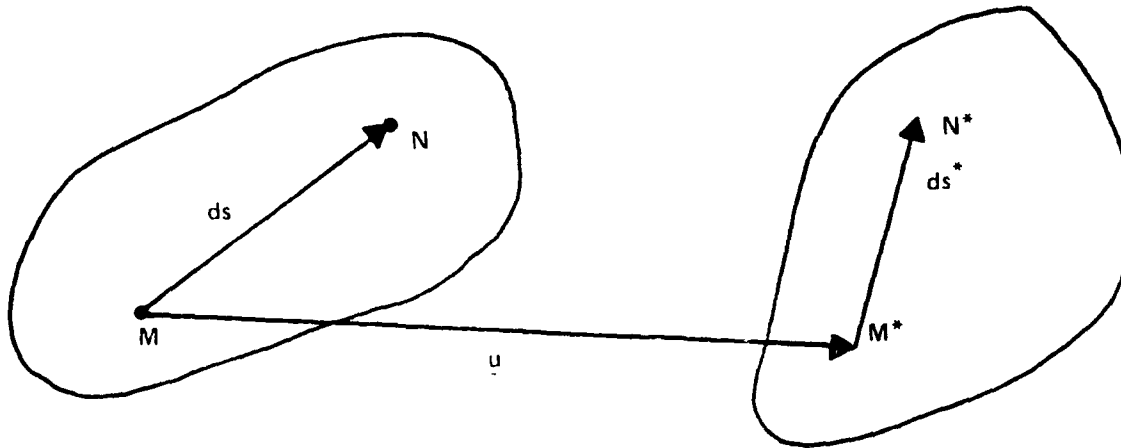


FIGURE 1. Segment MN Deforms to M^*N^* Through Displacement Vector \underline{u} .

Now consider a shell geometry that can be described by orthogonal curvilinear middle surface coordinates, ξ_1 and

ξ_2 , surface normal ζ , and radii of curvature, R_1 and R_2 as shown in Figure 2. For this geometry, the scale factor terms of Eqn (2) are given by,

$$h_1 = \alpha_1 (1 - \zeta/R_1), \quad h_2 = \alpha_2 (1 - \zeta/R_2), \quad h_3 = 1 \quad (3)$$

where α_γ ($\gamma=1,2$) are related to the elements of the surface metric [1].

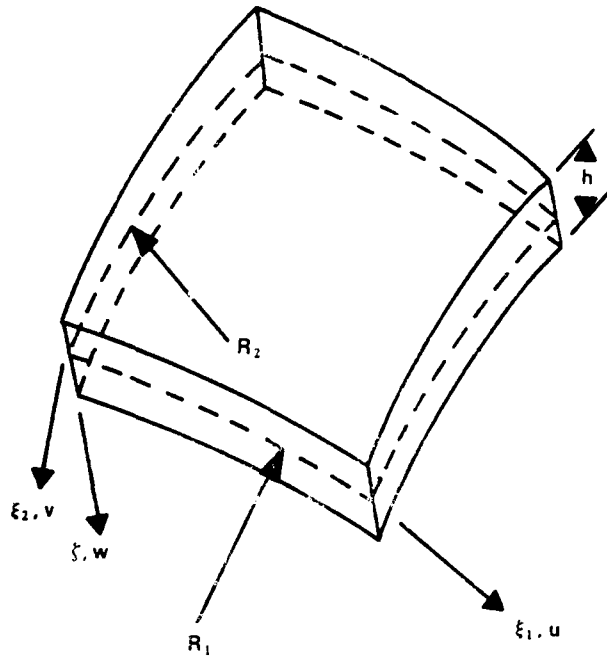


FIGURE 2. Arbitrary Shell Coordinate System.

For a body of volume V in equilibrium with prescribed forces on a part of its surface, S_1 , and prescribed geometric boundary conditions on the remaining surface, S_2 , that has undergone an infinitesimal virtual displacement, δu , we have,

$$\int_V (\sigma_{ij} \delta \epsilon_{ij} - P_k \delta u_k) dV - \int_{S_1} F_k \delta u_k dS = 0 \quad (4)$$

where, σ_{ij} are elements of the 2nd Piola-Kirchhoff stress tensor, ϵ_{ij} are defined in Eqn (2), P_k are components of prescribed body forces, and F_k are components of prescribed surface tractions [53]. Assuming the existence of a strain energy density function, W^* , small strain deformation, and a linear constitutive law, the principle of stationary potential energy can be stated as,

$$\delta \Pi_P = 0 \quad (5)$$

and if the forces vary neither in magnitude nor direction during virtual displacements,

$$\Pi_P = \int_V W^*(u_i) dV - \int_{S_1} F_i u_i dS \quad (6)$$

where $W^*(u_i) = 1/2 a_{ijkl} \epsilon_{ij} \epsilon_{kl}$, a_{ijkl} are elastic constants.

In Eqns (5,6), the strain energy density is written in terms of the displacement components by using Eqns (2,A1). The integrals are taken over the original, undeformed volume and surfaces consistent with a Lagrangian viewpoint. Additionally, the array of elasticity constants, a_{ijkl} , are defined with respect to the original configuration. [53]

All of the necessary tools have been introduced for a Lagrangian displacement based energy approach to solve elastic geometrically nonlinear shell problems. To develop shell strain displacement relations, one should first identify, respectively, the general 3-D curvilinear

coordinates y_1 , y_2 , and y_3 of Eqns (1,2,A1) with the shell coordinates, ξ_1 , ξ_2 , and ξ of Figure 2. Then, by defining kinematics that relate the middle surface displacements to the continuum displacements of the shell, strain displacement relations are written, and finally, the total potential energy expressed in terms of displacement using Eqns (5,6) is extremized with respect to displacement resulting in the equilibrium equations. The definition of the kinematics for these types of formulations is obviously very important. The assumptions that will eventually lead to general shell kinematics and a potential energy expression are next discussed.

Basic Assumptions

A geometrically nonlinear theory governing the shell is based on the following assumptions:

1. The shell is thin and therefore assume that it is in an approximate state of plane stress, i.e., the transverse normal stress is approximately equal to zero. This assumption effectively reduces the generally three dimensional behavior of the shell so that it can be described by the behavior of only a datum surface; this results in a 2-D approach.
2. The transverse shear stress distribution is parabolic through the shell thickness and vanishes on the top and bottom surfaces of the shell.

Because the shell is thin, in-plane stress tends to dominate the shell response under loading, i.e., the

transverse stresses are of lesser importance. However, it is well known that laminated thin flat plate response can be significantly influenced by transverse shear deformation. Similar results have been found for laminated shells [39,54]. Therefore, transverse shear stress is included in the present model, via a 2-D approach whereas, transverse normal stress is not. This approach is consistent with remarks made by Koiter [10,55] and John [56] who performed order of magnitude studies on the stresses in general shell geometries. Additionally, their results are seen to hold generally true in the elasticity solutions of both laminated flat plates by Pagano [57,58] and laminated shells in cylindrical bending by Ren [59].

3. The shell is restricted to small strains and consists of linear elastic laminated orthotropic material.

4. Exact Green's strain displacement relations are assumed for the in-plane strains ϵ_{11} , ϵ_{22} , and ϵ_{12} of Eqns (2,3) and linear strain displacement relations are assumed for the transverse strains ϵ_{23} and ϵ_{13} .

5. Since the shell is assumed thin, the normals to the middle surface are approximately inextensible, hence the transverse displacement is constant through the thickness. Consistent with the preceding assumption, retention of only linear strain displacement terms then gives $\epsilon_{33} = 0$.

Librescu [39], as mentioned, develops general shell equations based upon varying approximations in the magnitudes of both strain and the rotations differential

elements undergo during deformation. A consistent small strain, moderate rotation theory has nonlinear (not exact!) strain displacement relations for the in-plane strains yet linear relations for the transverse shear strains. The present approach can therefore be viewed as a small strain, simplified large rotation theory due to the exact in-plane strain assumption. The accuracy in rotation is limited by the linear (in displacement) assumption on the transverse shear strains.

Constitutive Relations

Materials consisting of unidirectional fibers embedded in a matrix are of interest in this study. For fibers aligned with the 1 material axis, we can assume that the material is transversely isotropic (engineering constants $E_2=E_3$ and $\nu_{12}=\nu_{13}$) with respect to planes parallel to the 2-3 plane [60]. In this case, the constitutive relation used in Eqn (6) becomes,

$$\begin{Bmatrix} \sigma_1 \\ \sigma_2 \\ \sigma_3 \\ \sigma_4 \\ \sigma_5 \\ \sigma_6 \end{Bmatrix} = \begin{bmatrix} C_{11} & C_{12} & C_{13} & 0 & 0 & 0 \\ C_{12} & C_{22} & C_{23} & 0 & 0 & 0 \\ C_{13} & C_{23} & C_{33} & 0 & 0 & 0 \\ 0 & 0 & 0 & C_{44} & 0 & 0 \\ 0 & 0 & 0 & 0 & C_{55} & 0 \\ 0 & 0 & 0 & 0 & 0 & C_{66} \end{bmatrix} \begin{Bmatrix} \epsilon_1 \\ \epsilon_2 \\ \epsilon_3 \\ \epsilon_4 \\ \epsilon_5 \\ \epsilon_6 \end{Bmatrix} \quad (7)$$

where contracted notation is introduced, i.e., $\sigma_i = \sigma_{ii}$ (no sum), $\sigma_4 = \sigma_{23}$, $\sigma_5 = \sigma_{13}$, $\sigma_6 = \sigma_{12}$, and $\epsilon_i = \epsilon_{ii}$ (no sum), $\epsilon_4 = 2\epsilon_{23}$, $\epsilon_5 = 2\epsilon_{13}$, $\epsilon_6 = 2\epsilon_{12}$.

Using assumption 1 ($\sigma_3 \cong 0$) in Eqn (7), solve for ϵ_3 .

$$\varepsilon_3 = -\frac{C_{13}}{C_{33}} \varepsilon_1 - \frac{C_{23}}{C_{33}} \varepsilon_2 \quad (8)$$

Substituting back into Eqn (7), ε_3 is eliminated, and the constitutive relations in material axes become,

$$\begin{Bmatrix} \sigma_1 \\ \sigma_2 \\ \sigma_6 \\ \sigma_4 \\ \sigma_5 \end{Bmatrix} = \begin{bmatrix} Q_{11} & Q_{12} & 0 & 0 & 0 \\ Q_{12} & Q_{22} & 0 & 0 & 0 \\ 0 & 0 & Q_{66} & 0 & 0 \\ 0 & 0 & 0 & Q_{44} & 0 \\ 0 & 0 & 0 & 0 & Q_{55} \end{bmatrix} \begin{Bmatrix} \varepsilon_1 \\ \varepsilon_2 \\ \varepsilon_6 \\ \varepsilon_4 \\ \varepsilon_5 \end{Bmatrix} \quad (9)$$

where $Q_{ij} = C_{ij} - \frac{C_{i3}C_{j3}}{C_{33}}$, and for transverse isotropy, it

is easily shown that, $Q_{11} = E_1/\Delta$, $Q_{12} = \nu_{21}E_2/\Delta$, $Q_{22} = E_2/\Delta$,

$Q_{66} = G_{12}$, $Q_{44} = G_{23}$, $Q_{55} = G_{13}$, $\Delta = 1 - \nu_{12}\nu_{21}$.

Consider a shell that is constructed of layers of the transversely isotropic material described by Eqn (9). Generally, the fibers of the k th individual layer or ply are oriented at an angle with respect to the middle surface shell coordinates ξ_1 and ξ_2 . Therefore, the constitutive relations of Eqn (9) for that ply must be transformed into shell coordinates resulting in Eqn (10).

$$\begin{Bmatrix} \sigma_1 \\ \sigma_2 \\ \sigma_6 \end{Bmatrix}^k = \begin{bmatrix} \bar{Q}_{11} & \bar{Q}_{12} & \bar{Q}_{16} \\ & \bar{Q}_{22} & \bar{Q}_{26} \\ & & \bar{Q}_{66} \end{bmatrix}^k \begin{Bmatrix} \epsilon_1 \\ \epsilon_2 \\ \epsilon_6 \end{Bmatrix} \quad (10)$$

$$\begin{Bmatrix} \sigma_4 \\ \sigma_5 \end{Bmatrix}^k = \begin{bmatrix} \bar{Q}_{44} & \bar{Q}_{45} \\ & \bar{Q}_{55} \end{bmatrix}^k \begin{Bmatrix} \epsilon_4 \\ \epsilon_5 \end{Bmatrix}$$

where, the \bar{Q}_{ij} ($i, j=1, 2, 6$) and \bar{Q}_{mn} ($m, n=4, 5$) are elements of symmetric arrays of transformed stiffnesses for the k th ply and σ_i , ϵ_i , σ_m , and ϵ_m are measured with respect to shell coordinates ξ_α and ζ .

Kinematics

Consider the following kinematics for the arbitrary shell described by orthogonal curvilinear coordinates, referring back to Figure 2 for conventions.

$$\begin{aligned} u_1(\xi_1, \xi_2, \zeta) &= u(1 - \zeta/R_1) + \zeta\psi_1 + \zeta^2\phi_1 + \zeta^3\gamma_1 + \zeta^4\theta_1 \\ u_2(\xi_1, \xi_2, \zeta) &= v(1 - \zeta/R_2) + \zeta\psi_2 + \zeta^2\phi_2 + \zeta^3\gamma_2 + \zeta^4\theta_2 \\ u_3(\xi_1, \xi_2) &= w \end{aligned} \quad (11)$$

where, u , v , w , ψ_α , ϕ_α , γ_α , and θ_α , are functions of ξ_1 and ξ_2 ; ψ_α are rotations of the normals and; ϕ_α , γ_α , θ_α , are functions to be determined such that σ_4 and σ_5 vanish on the top and bottom surfaces of the shell.

The assumed displacements of Eqn (11) are slightly more involved than those introduced for flat plates by [27]. For a plate, only third order terms in the thickness parameter,

ζ , were necessary to give the desired parabolic transverse stress distribution. Shell structures, due to their curved surfaces, however, have coupling between displacements that plates do not and the fourth order terms become necessary. The kinematics will ultimately closely resemble the plate kinematics that have been used in the literature. Additionally, Reddy [30] arrives at identical general shell kinematics as derived here but uses Sanders shell relations.

Keeping only linear displacement terms from Eqns (2,A1), the transverse shear strains become,

$$\begin{aligned}\epsilon_4 &= \frac{1}{h_2} (u_{3,2} + h_2 u_{2,3} - u_2 h_{2,3}) \\ \epsilon_5 &= \frac{1}{h_1} (u_{3,1} + h_1 u_{1,3} - u_1 h_{1,3})\end{aligned}\tag{12}$$

where $()_{,\alpha}$ ($\alpha=1,2$) refers to differentiation with respect to ξ_α and $()_{,3}$ refers to differentiation with respect to ζ .

Using Eqn (11) in the first of Eqn (12) and assuming zero transverse shear stress, and therefore, strain, on the shell boundaries (see Eqns (9,10)) the following is derived,

$$\begin{aligned}\phi_2 &= 0, \\ \theta_2 &= \frac{\gamma_2}{2R_2},\end{aligned}\tag{13}$$

$$\left[1 - \frac{h^2}{8R_2^2} \right] \gamma_2 \approx \gamma_2 = \frac{-4}{3h^2} \left(\psi_2 + \frac{w_{,2}}{\alpha_2} \right)$$

where h is the shell thickness, see Figure 2.

Assume, for the moment, that we have a fairly thick shell, i.e., let $R_2 = 5h$. In this case, the underlined term

in Eqn (13) is only .005 and therefore can be neglected compared to 1 as indicated. Furthermore, we can neglect the fourth order term (θ_2) of Eqns (11,13) since it is only 1/20 of the third order term. A similar exercise is applied to ϵ_5 giving for the general shell kinematics,

$$u_1(\xi_1, \xi_2, \zeta) = u(1 - \frac{\zeta}{R_1}) + \zeta \psi_1 + \zeta^3 k(\psi_1 + \frac{w_{,1}}{\alpha_1})$$

$$u_2(\xi_1, \xi_2, \zeta) = v(1 - \frac{\zeta}{R_2}) + \zeta \psi_2 + \zeta^3 k(\psi_2 + \frac{w_{,2}}{\alpha_2})$$

$$u_3(\xi_1, \xi_2) = w \tag{14}$$

where, $k = \frac{-4}{3h^2}$.

The rotation of the normal, ψ_α , is a result of bending deformation and therefore, the slope of the elastic curve, $w_{,\alpha}$, is always a combination of ψ_α and shear, β_α , as shown in Figure 3. For a flat plate, $\zeta/R_\alpha=0$ and $\alpha_\gamma = 1$ and Eqn (14) reduces to that used in the literature.

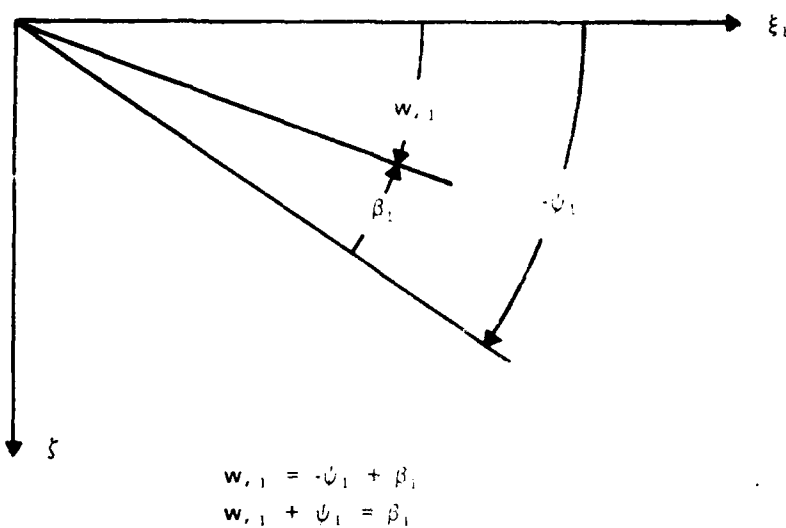
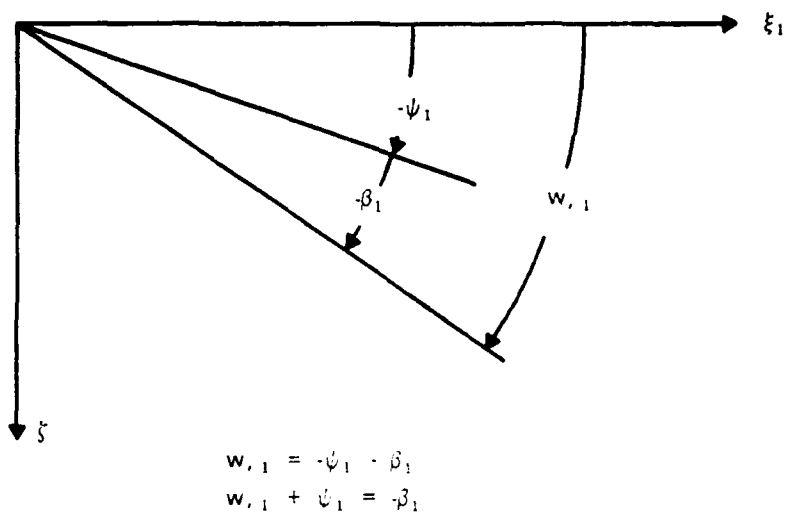


FIGURE 3. Slope of the Elastic Curve is Always a Combination of Bending and Shear.

Shell Strain Displacement Relations

The kinematics of Eqn (14) next define the general shell strain displacement relations using Eqn (A1) as given in Eqn (15).

$$\epsilon_i = \epsilon_i^0 + \zeta^p \kappa_{ip}, \quad i=1,2,6 \quad (15)$$

p sum 1 to 7

$$\epsilon_m = \epsilon_m^0 + \zeta^2 \kappa_{m2}, \quad m=4,5$$

where, ϵ_i^0 , κ_{i1} through κ_{i7} , ϵ_m^0 , κ_{m2} are shown in the Appendix, Eqns (A2-A6), specialized for cylindrical coordinates. Note that the convention on i (and j) has been changed so that instead of taking on values 1,2, or 3, they now represent the values 1,2, and 6. This will always be the case from this point on. The first subscript of κ_{ip} refers to the strain component 1,2, or, 6 and the second subscript refers to the power of ζ it multiplies. The ϵ_i^0 and the κ_{i1} through κ_{i7} terms consist of displacement expressions that are dependent only on the surface parameters ξ_1 and ξ_2 .

In developing the 2-D theory, it is convenient to define the strains such that the strain terms multiplying the ζ 's in the expressions of Eqn (15) are functions only of the in-plane parameters, ξ_1 and ξ_2 . Therefore, in arriving at Eqn (15), binomial series expansions such as those shown in Eqn (16) were used for this purpose. Terms similar to the left hand sides of Eqn (16) result due to the shell scale factors, i.e., those terms in Eqns (A2-A4) that are

functions of h_i . For the thick shell case where $R_\alpha = 5h$ and $\zeta = h/2$, the first two terms on the right hand sides for each expression in Eqn (16) represent 99% and 97%, respectively, of the total on the left hand sides. Consequently, series expansions as in Eqn (16) and similar expansions are truncated after the first order ζ terms.

$$\frac{1}{1 - \frac{\zeta}{R_\alpha}} = 1 + \frac{\zeta}{R_\alpha} + \frac{\zeta^2}{R_\alpha^2(1 - \zeta/R_\alpha)} \quad (16)$$

$$\frac{1}{\left(1 - \frac{\zeta}{R_1}\right) \left(1 - \frac{\zeta}{R_2}\right)} = 1 + \zeta \left[\frac{1}{R_1} + \frac{1}{R_2} \right] + \text{rem}$$

For simplicity, in arriving at the transverse shear strains of Eqn (15), the cubic term found as a result of Eqns (12,14) is neglected as small using the $R_\alpha = 5h$ argument as before. This results in a symmetric transverse shear strain and stress distribution about the midplane of the shell. In reality however, as the shell becomes thicker, the transverse shear stress tends to become less symmetric about the midplane.

Shell Potential Energy

From Eqn (6), let

$$\Pi_p = U + V \quad (17)$$

where, U is the internal strain energy, and V is the work

done by the external forces.

Eqns (10,17,15) then give for the internal strain energy of the arbitrary shell,

$$\begin{aligned}
 U_1 = \frac{1}{2} \int_{\Omega} \int_h & \left[\bar{Q}_{11} (\epsilon_1^\circ + \zeta^p \kappa_{1p})^2 + \bar{Q}_{22} (\epsilon_2^\circ + \zeta^p \kappa_{2p})^2 \right. \\
 & + 2\bar{Q}_{12} (\epsilon_1^\circ + \zeta^p \kappa_{1p}) (\epsilon_2^\circ + \zeta^p \kappa_{2p}) + \bar{Q}_{66} (\epsilon_6^\circ + \zeta^p \kappa_{6p})^2 \\
 & + 2\bar{Q}_{16} (\epsilon_1^\circ + \zeta^p \kappa_{1p}) (\epsilon_6^\circ + \zeta^p \kappa_{6p}) \\
 & \left. + 2\bar{Q}_{26} (\epsilon_2^\circ + \zeta^p \kappa_{2p}) (\epsilon_6^\circ + \zeta^p \kappa_{6p}) \right] d\zeta d\Omega, \quad (18)
 \end{aligned}$$

$$\begin{aligned}
 U_2 = \frac{1}{2} \int_{\Omega} \int_h & \left[\bar{Q}_{44} (\epsilon_4^\circ + \zeta^2 \kappa_{42})^2 + \bar{Q}_{55} (\epsilon_5^\circ + \zeta^2 \kappa_{52})^2 \right. \\
 & \left. + 2\bar{Q}_{45} (\epsilon_4^\circ + \zeta^2 \kappa_{42}) (\epsilon_5^\circ + \zeta^2 \kappa_{52}) \right] d\zeta d\Omega
 \end{aligned}$$

where, $U = U_1 + U_2$, $p, r = 1, 2, 3, 4, 5, 6, 7$, \bar{Q}_{ij} generally vary as a function of ζ since a laminate is constructed of plies with various fiber orientations, and, Ω represents the shell middle surface.

Manipulations of Eqn (18) are facilitated if the following quantities are defined. From Eqn (15), let

$$\xi = \xi^\circ + \kappa \mathcal{Z} \quad (19)$$

where,

$$\mathbf{\epsilon} = \begin{Bmatrix} \epsilon_1 \\ \epsilon_2 \\ \epsilon_6 \end{Bmatrix}, \quad \mathbf{\epsilon}^* = \begin{Bmatrix} \epsilon_1^* \\ \epsilon_2^* \\ \epsilon_6^* \end{Bmatrix}, \quad \mathbf{\kappa} = \begin{bmatrix} \kappa_{11} & \kappa_{12} & \dots & \kappa_{17} \\ \kappa_{21} & \kappa_{22} & \dots & \kappa_{27} \\ \kappa_{61} & \kappa_{62} & \dots & \kappa_{67} \end{bmatrix}, \quad \mathbf{\zeta} = \begin{Bmatrix} \zeta \\ \zeta^2 \\ \vdots \\ \zeta^7 \end{Bmatrix}$$

Using Eqn (19) in the first of Eqn (18), we get,

$$U_1 = \frac{1}{2} \int_{\Omega} \int_h (\mathbf{Q} \mathbf{\epsilon})^T \mathbf{\epsilon} \, d\zeta \, d\Omega \quad (20)$$

$$= \frac{1}{2} \int_{\Omega} \int_h \left\{ \epsilon_j^* \epsilon_i^* \bar{Q}_{ij} + 2 \epsilon_j^* \bar{Q}_{ij} \kappa_{ip} \zeta^p + \kappa_{jp} \kappa_{ir} \bar{Q}_{ij} \zeta^{p+r} \right\} d\zeta \, d\Omega$$

where, $\mathbf{Q} = \begin{bmatrix} \bar{Q}_{11} & \bar{Q}_{12} & \bar{Q}_{16} \\ & \bar{Q}_{22} & \bar{Q}_{26} \\ & & \bar{Q}_{66} \end{bmatrix}^k$, $i, j = 1, 2, 6$ and p, r sum 1 to 7.
superscript τ = transpose

The second integral of Eqn (20) hints at the complexity of the in-plane strain energy of the shell. The energy is comprised of many strain squared terms due to summations on up to four different indices. Finally, Eqn (20) is concisely written in terms of an area integral representing the shell midsurface as shown in Eqn (21) where the ζ dependence has been integrated by defining a series of elasticity arrays shown in Eqn (22). The u_k of Eqn (21) are written in terms of strain components and elements of the elasticity arrays in the Appendix, Eqn (A7).

$$U_1 = \frac{1}{2} \int_{\Omega} (u_1 + u_2 + u_3) d\Omega \quad (21)$$

$$\begin{aligned} & [A_{ij}, B_{ij}, D_{ij}, E_{ij}, F_{ij}, G_{ij}, H_{ij}, I_{ij}, J_{ij}, K_{ij}, \\ & L_{ij}, P_{ij}, R_{ij}, S_{ij}, T_{ij}] = \\ & \int_h \bar{Q}_{ij} [1, \zeta, \zeta^2, \zeta^3, \zeta^4, \zeta^5, \zeta^6, \zeta^7, \zeta^8, \zeta^9, \zeta^{10}, \zeta^{11}, \zeta^{12}, \zeta^{13}, \zeta^{14}] d\zeta \end{aligned} \quad (22)$$

where $i, j = 1, 2$, and 6 .

A similar manipulation is performed on the second of Eqn (18), the shear terms, giving,

$$U_2 = \frac{1}{2} \int_{\Omega} (\varepsilon_m^0 \varepsilon_n^0 A_{mn} + 2 \varepsilon_n^0 \kappa_{m2} D_{mn} + \kappa_{n2} \kappa_{m2} F_{mn}) d\Omega \quad (23)$$

and, with $m, n = 4, 5$,

$$[A_{mn}, D_{mn}, F_{mn}] = \int_h \bar{Q}_{mn} [1, \zeta^2, \zeta^4] d\zeta \quad (24)$$

Primarily due to the assumed nonlinearity, many new elasticity arrays are shown above. The energy terms that contain the higher order elasticity constants are also multiplied by powers of $k = -4/3h^2$ (see Eqn (14)). Because of the squared shell thickness term in the denominator of k , the energy terms are not as many orders of magnitude apart as Eqn (22) may at first indicate. For example, the D_{ij} , F_{ij} , and H_{ij} energy terms are all the same order of magnitude in h or ζ despite 4 orders of magnitude difference in the definitions of the elasticity arrays given in Eqn

(22).

In a general geometrically nonlinear analysis, the energy due to the externally applied loads contains nonlinear displacement terms. These arise when, because of large rotations, the applied loading develops higher order coupling components in coordinate directions where no loading originally existed. As discussed by Brush and Almroth [35], these higher order terms give potential energy contributions that are negligibly small for the cases of intermediate nonlinearity, i.e., moderate rotations. However, the large rotational case generally must account for them. If the loading is actually a prescription of displacement, the higher order nonlinear loading terms need not be included since applied loading is zero. This alternative simpler approach is taken here.

In summary, Eqn (21,23) with Eqns (A7,22,24,15,A2-A6), give the total potential energy of the arbitrary shell, where a specific shell geometry is defined by specifying the scale factor terms of Eqn (3). This expression is then extremized with respect to the displacements giving the equilibrium equations. The result of the extremization is five coupled nonlinear partial differential equations. The present approach gives nonlinear extensional terms, i.e., terms in A_{ij} , as well as nonlinear terms in D_{ij} through T_{ij} due to the nonlinearity in the curvature terms (κ_{ip}) of Eqn (15). The moderate rotational theories retain in the strain displacement relations nonlinear displacement terms only in

the transverse displacement, w , as a result of assuming that the rotations are small compared to unity [36] This results in nonlinearity in the equilibrium equations in the extensional A_{ij} terms only.

III. Finite Element Solution

The variation of the potential energy, Π_p , of the discretized domain gives coupled nonlinear algebraic equations where the unknowns are the values of displacement at the nodes. In a generally nonlinear analysis, these equations are not usually solved directly, but instead, are linearized and solved by incremental/iterative methods. The linearized equations are found by effectively carrying out an additional differentiation of Π_p with respect to the displacements. The manipulations that follow give a convenient form for Π_p such that the variation and linearization are straight forward to accomplish. Afterward, a 36 degree of freedom (dof) curved element is discussed.

Element Independent Formulation

We seek a form for the potential energy, Π_p , shown in Eqn (25), such that the first variation, $\delta\Pi_p$, is given by Eqn (26) and the linearized incremental/iterative equations are given in the last of Eqn (28). Eqn (28) is found from Eqn (26) by expansion of the equilibrium equations, $F(q)$, into a Taylor series about a small Δq and truncating as shown in Eqn (27).

$$\Pi_p = \frac{q^T}{2} \left[K + \frac{N_1}{3} + \frac{N_2}{6} \right] q - q^T R \quad (25)$$

$$\delta\Pi_p = \delta q^T \left[\left\{ K + \frac{N_1}{2} + \frac{N_2}{3} \right\} q - R \right] = \delta q^T F(q) = 0 \quad (26)$$

where, q is a column array of nodal displacements, R is a column array of nodal loads, K is an array of constant stiffness coefficients, N_1 is an array of stiffness coefficients that are linear in displacement, N_2 is an array of stiffness coefficients that are quadratic in displacement.

From Eqn (26), for arbitrary and independent δq , $F(q) = 0$, then,

$$F(q + \Delta q) = F(q) + \frac{\partial F}{\partial q} \Delta q + \dots = 0 \quad (27)$$

$$\frac{\partial F}{\partial q} \Delta q = [K + N_1 + N_2] \Delta q \equiv K_T \Delta q = -F(q) \quad (28)$$

where K_T is the tangent stiffness matrix.

Eqn (28) gives solutions in an iterative manner via a Newton-Raphson technique. The current values of the elements of q are substituted into N_1 and N_2 resulting in an array of constants for K_T . The set of linear equations are then solved for Δq , which is then added to q giving the updated nodal displacements. Assuming the solution is not yet converged, the right hand side (RHS) of Eqn (28) is nonzero. Iteration continues until $F(q)$ becomes arbitrarily small signifying equilibrium has been satisfied.

The preceding general development assumed a certain formalism in the definitions of the arrays, K , N_1 , and N_2 in Π_p of Eqn (25) such that these terms repeat themselves in the first variation of Π_p (Eqn (26)) and again in the Taylor series expansion that gave the incremental equations (Eqn

(28)). Ensuring this formalism will greatly decrease the required number of algebraic manipulations since once K , N_1 , and N_2 are formed in the Π_p expression of Eqn (25), the variation and linearization processes become straight forward. Additionally, fewer programming lines are needed since the same arrays are present in both the equilibrium and incremental equations and hence need be calculated only once per iteration in solving Eqn (28).

Rajasekaran and Murray [61] outline a procedure that will give the desired repetition and also symmetry of the three components, K , N_1 , and N_2 , that comprise K_T . Some generalizations are used in the present case. We start by dividing each strain component of Eqn (15) into linear and nonlinear parts as shown in Eqn (29).

$$e_i^o = {}_oL_i^T d + \frac{1}{2} d^T {}_oH_i d \quad (29)$$

$$x_{ip} = {}_pL_i^T d + \frac{1}{2} d^T {}_pH_i d$$

where, ${}_jL_i$ ($j = 0, 1, 2, \dots, 7$) are column arrays, ${}_jH_i$ are symmetric matrices, d is the displacement gradient vector, $i = 1, 2, 6$ and $p = 1$ to 7 , as before, ${}_pL_i$ for $p = 5, 6, 7$ contain all zeroes.

The displacement gradient vector contains the unique displacement terms that define the strain components in Eqn (15). Since there are 18 unique displacement terms in Eqn (15), the vector, d , is an 18×1 array as shown in Eqn (30). The way in which the elements of d are approximated defines

the specific element type, i.e., number of dof, shape functions, etc. This elemental definition is done independent of the repeating formalism of Eqns (25,26,28). The ${}_jL_i$ and ${}_jH_i$ therefore, are, 18x1 and 18x18 arrays respectively, and contain constants.

$$d^T = \left\{ u \ u_{,1} \ u_{,2} \ v \ v_{,1} \ v_{,2} \ w \ w_{,1} \ w_{,2} \ w_{,11} \ w_{,22} \ w_{,12} \right. \\ \left. \psi_1 \ \psi_{1,1} \ \psi_{1,2} \ \psi_2 \ \psi_{2,1} \ \psi_{2,2} \right\} \quad (30)$$

Next, Eqn (30) is substituted into the internal strain energy of Eqn (21) giving for the in-plane energy expression, i.e., those energy terms due to ϵ_1 , ϵ_2 , and ϵ_6 ,

$$U_1 = \frac{1}{2} \int_{\Omega} d^T \left[\tilde{K} + \tilde{N}_1 + \frac{1}{4} \tilde{N}_2 \right] d \ d\Omega \quad (31)$$

where \tilde{K} , \tilde{N}_1 , \tilde{N}_2 are symmetric 18x18 arrays given in Eqns (A8-A10) in the Appendix.

Each term of the \tilde{K} , \tilde{N}_1 , and \tilde{N}_2 expressions of Eqns (A8-A10) represents nine terms due to the summation convention on i and j. Each of these nine terms results in an 18x18 array that is premultiplied by a scalar elasticity element, see also Eqn (22). Eqns (32) show one representative term from \tilde{K} , \tilde{N}_1 , \tilde{N}_2 , respectively.

$$\begin{aligned}
\tilde{K} : & \quad A_{11} \begin{bmatrix} oL_1 & oL_1^T \\ 1 \times 1 & 18 \times 1 & 1 \times 18 \end{bmatrix} \\
\tilde{N}_1 : & \quad A_{11} \begin{bmatrix} oL_1 & d^T & oH_1 \\ 1 \times 1 & 18 \times 1 & 1 \times 18 & 18 \times 18 \end{bmatrix} \\
\tilde{N}_2 : & \quad A_{11} \begin{bmatrix} oX_1 & d & d^T & oH_1 \\ 1 \times 1 & 18 \times 18 & 18 \times 1 & 1 \times 18 & 18 \times 18 \end{bmatrix}
\end{aligned} \tag{32}$$

As explained by [61], the desired formalism of Eqns (25,26,28), will not be exhibited using the terms as defined in Eqns (31,32,A8-A10). That is, if the first variation were carried through on Eqn (31) with the \tilde{K} , \tilde{N}_1 , and \tilde{N}_2 as defined in Eqns (A8-A10), totally new terms would result. Similarly, the formation of the linearized incremental/iterative equations would result in still different terms. To avoid these tedious manipulations, we seek equivalent energy forms for \tilde{K} , \tilde{N}_1 , and \tilde{N}_2 such that repeating symmetric terms are present in the three expressions for Π_p , $F(q)$, and K_T , i.e., Eqns (25,26,28).

Each of the energy terms of \tilde{N}_1 are of the form shown on the left hand side (LHS) of Eqn (33) where, C_{ij} refers to the elements from any of the elasticity arrays, A_{ij} to T_{ij} , $p,r = 0$ to 7 and $i,j=1,2,6$ as before. As suggested by Ref [61], if each of these terms is replaced by the terms of the RHS of Eqn (33), the desired repeating formalism of Eqns (25,26,28), will apply.

$$\frac{1}{2} \int_{\Omega} d^T C_{ij} p L_i d^T r H_j d d\Omega =$$

$$\frac{1}{6} \int_{\Omega} d^T C_{ij} \left[p L_i d^T r H_j + d^T p L_i r H_j + r H_i d p L_j^T \right] d d\Omega$$

(33)

Using the underlined term from \tilde{N}_1 of Eqn (A9) with the Eqn (33) substitution, the first variation is as shown in Eqn (34). It is stressed that this term is representative of all the \tilde{N}_1 terms of Eqn (A9).

$$\delta \left\{ \frac{1}{2} \int_{\Omega} d^T B_{ij} o L_i d^T i H_j d d\Omega \right\} =$$

$$\delta \left\{ \frac{1}{6} \int_{\Omega} d^T B_{ij} \left[o L_i d^T i H_j + d^T o L_i i H_j + i H_i d o L_j^T \right] d d\Omega \right\}$$

$$= \frac{1}{6} \int_{\Omega} B_{ij} \left\{ \left(\delta d^T o L_i d^T i H_j d + d^T o L_i \delta d^T i H_j d + d^T o L_i d^T i H_j \delta d \right) \right. \\ \left. + \left(\delta d^T d^T o L_i i H_j d + d^T \delta d^T o L_i i H_j d + d^T d^T o L_i i H_j \delta d \right) \right. \\ \left. + \left(\delta d^T i H_i d o L_j^T d + d^T i H_i \delta d o L_j^T d + d^T i H_i d o L_j^T \delta d \right) \right\} d\Omega$$

$$= \frac{1}{6} \int_{\Omega} B_{ij} \delta d^T \left[3 o L_i d^T i H_j + 3 d^T o L_i i H_j + 3 i H_i d o L_j^T \right] d d\Omega$$

(34)

A comparison of the terms in the second and final lines of Eqn (34) shows that the variation of the RHS of Eqn (33) gives a repeating form. The final result of Eqn (34) is

expanded into unabridged form in Eqn (35). In a similar fashion, we can show that the derivation of the linearized incremental/iterative equations (Eqn (28)) also results in similar repeating forms.

$$\begin{aligned} \frac{1}{6} \int_{\Omega} \left\{ B_{11} \delta d^T \left[3_0 L_1 d^T H_1 + 3 d^T_0 L_1 H_1 + 3_1 H_1 d_0 L_1^T \right] d \right. \\ + B_{12} \delta d^T \left[3_0 L_1 d^T H_2 + 3 d^T_0 L_1 H_2 + 3_1 H_1 d_0 L_2^T \right] d \\ + \dots \\ \left. + B_{66} \delta d^T \left[3_0 L_6 d^T H_6 + 3 d^T_0 L_6 H_6 + 3_1 H_6 d_0 L_6^T \right] d \right\} d\Omega \end{aligned} \quad (35)$$

Each of the terms of the \tilde{K} and \tilde{N}_2 arrays are of the general forms of the LHS of Eqn (36). In Eqn (36), two forms for both \tilde{K} and \tilde{N}_2 are shown. With the C_{ij} once again referring to elements from any of the elasticity arrays, the LHS are those energy terms from Eqns (31.A8,A10), that do not repeat in deriving the equilibrium and the linearized incremental/iterative equations. If each is replaced by the corresponding RHS of Eqn (36) then the formalism of Eqns (25,26,28) is easily shown similarly to the \tilde{N}_1 example of Eqns (33,34,35). The first substitutions shown in Eqn (36) for each of the arrays \tilde{K} and \tilde{N}_2 are similar to those of Ref [61] and the second substitutions are unique generalizations thereof.

From \tilde{K} :

$$\frac{1}{2} \int_{\Omega} d^T C_{ij} p^L_i p^L_j d d\Omega \quad (\text{no sum on } p) = \text{no change}$$

$$\frac{1}{2} \int_{\Omega} d^T 2C_{ij} p^L_i r^L_j d d\Omega =$$

$$\frac{1}{2} \int_{\Omega} d^T C_{ij} \left[p^L_i r^L_j + r^L_i p^L_j \right] d d\Omega \quad (p \neq r)$$

From \tilde{N}_2 :

$$\begin{aligned} \frac{1}{8} \int_{\Omega} d^T C_{ij} p^H_i d d^T p^H_j d d\Omega &= \frac{1}{12} \int_{\Omega} d^T C_{ij} \left[p^H_i d d^T p^H_j \right. \\ &\quad \left. + \frac{1}{2} d^T p^H_j d p^H_i \right] d d\Omega \quad (\text{no sum on } p) \end{aligned}$$

$$\begin{aligned} \frac{1}{8} \int_{\Omega} d^T C_{ij} r^H_i d d^T p^H_j d d\Omega &= \frac{1}{8} \int_{\Omega} \frac{d^T}{3} C_{ij} \left[r^H_i d d^T p^H_j \right. \\ &\quad \left. + \frac{1}{2} d^T r^H_i d p^H_j + p^H_i d d^T r^H_j + \frac{1}{2} d^T p^H_i d r^H_j \right] d d\Omega \quad (p \neq r) \end{aligned}$$

(36)

Based on Eqns (33,36), Eqn (31) can now be rewritten as in Eqn (37).

$$\begin{aligned} U_1 &= \frac{1}{2} \int_{\Omega} d^T \left[\tilde{K} + \tilde{N}_1 + \frac{1}{4} \tilde{N}_2 \right] d d\Omega \\ &= \frac{1}{2} \int_{\Omega} d^T \left[\hat{K} + \frac{\hat{N}_1}{3} + \frac{\hat{N}_2}{6} \right] d d\Omega \end{aligned} \quad (37)$$

where the elements of the arrays \hat{K} , \hat{N}_1 , and \hat{N}_2 are found from the \tilde{K} , \tilde{N}_1 , and \tilde{N}_2 of Eqn (A8-A10) by making all of the aforementioned substitutions of Eqns (33,36).

The transverse shear energy terms of Eqns (18,23,24) are handled in a totally analogous manner only much more simply since transverse shear strains are linear in displacement and hence any J_m^H terms are zero arrays and therefore not needed. Analogous to Eqn (29), the transverse shear strains of Eqn (15) are written below in Eqn (38).

$$\begin{aligned} \epsilon_m^o &= {}_o S_m^T d \\ \kappa_{2m} &= {}_2 S_m^T d \end{aligned} \quad (38)$$

where ${}_o S_m$ and ${}_2 S_m$ ($m=4,5$) are 18×1 arrays similar to the J_{L_i} of Eqn (29).

Due to the assumed linearity of these strains, there are additional energy terms from the transverse shear strains only for \tilde{K} of Eqn (31). These additional terms are found from Eqns (23,24,38) and are shown below in Eqn (39). The equivalent repeating forms that are added to \hat{K} of Eqn (37) are found via Eqn (36) as with the in-plane energy terms only now using the J_m^S arrays instead of the J_{L_i} arrays.

$$\frac{1}{2} \int_{\Omega} d^T (A_{mn} {}_o S_m {}_o S_n^T + 2D_{mn} {}_o S_m {}_2 S_n^T + F_{mn} {}_2 S_m {}_2 S_n^T) d \Omega \quad (39)$$

where $m, n = 4, 5$ as before.

The finite element is defined by the specific interpolation functions used to approximate the elements of

the displacement gradient vector, d . To this end, approximate the continuum displacements by shape functions and the nodal displacements in Eqn (40).

$$u = N q \quad (40)$$

where, u is the vector of continuum displacements, N is an array of interpolation or shape functions, q are the nodal values of displacements as before. Next, the displacement gradient vector, d , is approximated using Eqn (40) as shown below in Eqn (41).

$$d = D q \quad (41)$$

where D is the array of shape functions and their derivatives. Substituting Eqn (41) into the final expression of Eqn (37) including the transverse shear terms, then finally gives Eqn (25) for the potential energy, where in Eqn (42) we can now identify,

$$K = \int_{\Omega} D^T \hat{K} D d\Omega, \quad N_1 = \int_{\Omega} D^T \hat{N}_1 D d\Omega, \quad N_2 = \int_{\Omega} D^T \hat{N}_2 D d\Omega \quad (42)$$

Note that N_1 and N_2 are actually functions of the elements of d not q (see Eqn (36)) so that in practice, Eqn (41) is employed prior to Eqn (28) in the solution process. The terms of Eqns (25,26,28) are now defined, except for D which depends on the specific elemental definition and will be discussed in the next section.

The stiffness arrays, \hat{K} , \hat{N}_1 , and \hat{N}_2 are formed based on literally hundreds of 18×1 , 18×18 , and 1×18 symbolic matrix multiplications, see Eqn (A8-A10) with Eqns (33,36)

substitutions. These multiplications are impractical to carry out by hand; consequently, the symbolic manipulator code, MACSYMA, was employed. Additionally, MACSYMA can convert the resulting expressions into FORTRAN statements. Since these arrays are independent of element definition, subroutines are very easily implemented that calculate the entries of \hat{K} , \hat{N}_1 , and \hat{N}_2 where elemental information is included separately through \mathcal{D} .

In the finite element solution procedure, the stiffness of each element is calculated individually and added into a global stiffness array. In this way, the result of Eqns (25,42) equivalently represents the potential energy of an individual element, where the total Π_p is found by summing the energies from each element.

36 Degree of Freedom Curved Cylindrical Shell Element

The results from above are next used in the definition of a curved cylindrical shell finite element. The potential energy expression for the shell, Eqn (17) with cylindrical shell specializations for the strain quantities, Eqns (A2-A6), requires C^0 continuity for u , v , ψ_1 , and ψ_2 and C^1 continuity for w [62]. The simplest approach would be a curved shell element derived from Π_p with bilinear interpolation for u , v , ψ_1 , and ψ_2 and cubic Hermitian interpolation for w , w_1 , and w_2 resulting in a 4 noded 28 degree of freedom (dof) curved rectangular element. However, the in-plane continuum displacement dof, u and v , are coupled to the transverse displacement dof to a much

greater degree in the cylindrical shell compared to a flat plate due to the nonzero curvature in the circumferential direction of the former. Indeed, in a linear analysis, u and v are decoupled from the remaining dof for a flat plate. Consequently, it is felt that linear approximations for these variables, though quite adequate for a flat plate, are too simple for the shell, especially for cases where membrane action is significant. Therefore, assuming quadratic approximations for the in-plane dof u and v , and adding four nodes located at the midsides of the element, results in an eight noded 36 dof element, see Figure 4.

Although an element with this function assumed for w is nonconforming, it will pass the patch test and therefore converges as the mesh is refined [63]. However, monotonic convergence from a stiffer solution can no longer be expected as in a conforming elemental formulation. This incompatibility, however, is not nearly as significant for the present formulation as it is for simpler ones, e.g., Kirchhoff plate elements. Recall the present case includes parabolic transverse shear distribution through the thickness. For example, the shear rotation, β_1 , is equal to a combination of $w_{,1}$ and the bending rotation, ψ_1 , see Figure 3. For the limiting thin plate and shell situation, we would expect zero shear rotation and the incompatibility, in effect, disappears since $w_{,1} = \psi_1$ where ψ_1 use compatible approximations. This is not true for Kirchhoff elements with nonconforming w approximations. It should be pointed

out that this new element apparently does not suffer from the locking phenomenon usually encountered in shell element development [54].

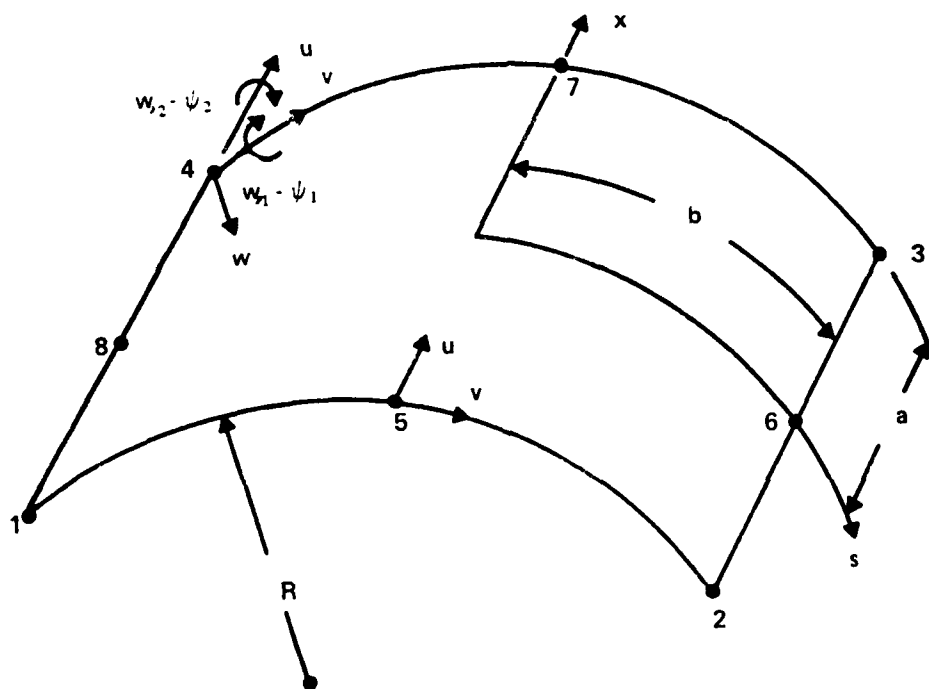


FIGURE 4. 36 dof Rectangular Shell Element. Corner Nodes have 7 dof, Midside Nodes have 2 dof.

IV. Laminated Shell in Cylindrical Bending

In linear analyses, the arrays N_1 and N_2 of Eqn (26) are not used and the equilibrium equations become those given in Eqn (43). Eqn (43) represents a system of simultaneous algebraic equations in the nodal unknowns, q , and are solved by gaussian elimination. All elemental stiffnesses are integrated exactly using 4x4 point gaussian quadrature. Upon solving Eqn (43) for q , the elemental stresses are calculated at the outermost gauss points, i.e., those nearest the corners of each element. The stresses are not extrapolated to give the nodal values.

$$K q = R \quad (43)$$

The present theoretical approach and finite element casting is applied to a laminated circular cylindrical shell in cylindrical bending, see Figures 5 and 6 for geometry and material properties. The shell has infinite length in the x -direction; is simply supported at the two ends, $s=0$ and L ; and is subjected to a sinusoidal normal pressure loading. The direction of the pressure, $q(x,s)$, will induce compressive stress (σ_2) on the bottom of the shell ($\zeta > 0$) and tensile stress on the top ($\zeta < 0$).

The infinite shell geometry and simple supports are represented by the boundary conditions of Eqn (44). Additionally, due to symmetry, only one half of the shell length circumferentially is modelled and the halves are matched by the boundary conditions at $s=L/2$. The length,

B, shown in Figure 6 is determined such that all elements have an aspect ratio of one. The pressure loading is given in Eqn (45).

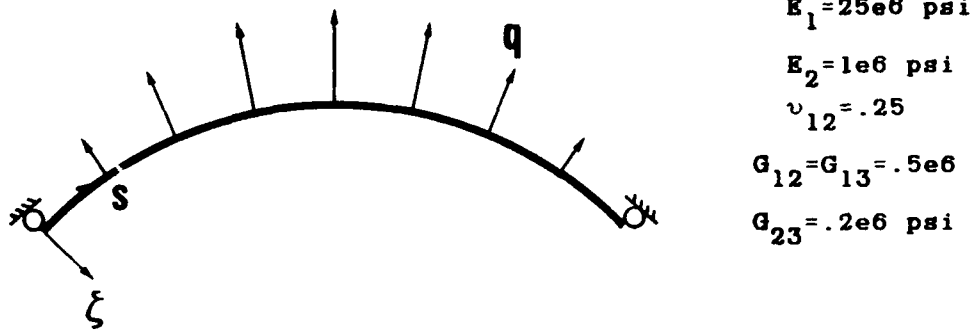


FIGURE 5. Cylindrical Shell Geometry, Radius $R=10''$, Arc length $L=10.472''$, thickness h .

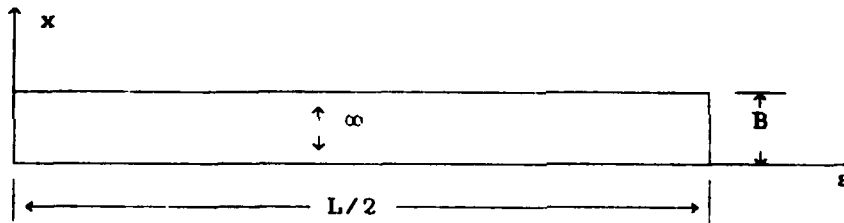


FIGURE 6. Planform of Shell Showing one half Circumferential Length, $L/2$, and Discretization Length, B .

$$\begin{array}{lll}
 \text{along } x = 0, B & u = w_{,1} = \psi_1 = 0 & \\
 s = 0 & w = w_{,1} = 0 & (44) \\
 s = L/2 & v = w_{,2} = \psi_2 = 0 &
 \end{array}$$

$$q(x, s, 0) = q_0 \sin(\pi s/L) \quad (45)$$

Results are generated for [90] unidirectional and [90/0/90] cross ply laminates and compared to exact elasticity solutions given by Ren [59]. Calculated

displacements and stresses are nondimensionalized as shown in Eqn (46). The transverse displacement, w , and the inplane stresses, σ_1 and σ_2 , are taken from the center of the laminate, i.e., at $s=L/2$. The transverse shear stress, σ_4 , and the circumferential displacement, u_2 , are taken from the left side of the laminate, i.e., at $s=0$. The sign of the quantities of Eqn (46) is opposite that given by Ren in some cases since the respective coordinate systems are different. The changes are made so that the physical and nondimensionalized quantities have the same sign.

Regular meshes of 5, 10, and 20 elements give the nondimensionalized transverse displacement, \bar{w} , for $S=100$, [90] laminate, shown in Table 1. Also shown is the exact value. The Table shows that the 1x20 mesh (x by s) results converge. Using the 1x20 mesh, further displacement and stress results are generated and shown in Tables 2-9. Two values are given for $\bar{\sigma}_4$ in Tables 5 and 9. The transverse shear stress varies very rapidly near the support for the thinner shell geometries and therefore to get an accurate value, a mesh refinement becomes necessary. The value in the Tables indicated by an asterisk is the stress calculated based on a 1x20 mesh that has smaller elements nearer the support. As can be seen, this generally gives a better value of $\bar{\sigma}_4$ for the thin cases but is unchanged for the thicker laminates where the shear stress has a smaller gradient near the support.

$$(\bar{\sigma}_1, \bar{\sigma}_2) = \frac{(\sigma_1, \sigma_2)}{-q_0 S^2}, \quad \bar{\sigma}_4 = \left| \frac{\sigma_4}{q_0 S} \right| \quad (46)$$

$$\bar{w} = \frac{10E_2 w}{q_0 h S^4}, \quad \bar{v} = \frac{100E_2 u_2}{q_0 h S^3}, \quad S=R/h, \quad \bar{z}=\zeta/h$$

Mesh (x by s)	\bar{w}	Exact (Ren)
1x5	.0727	
1x10	.0749	
1x20	.0751	.0755

TABLE 1. Convergence of Transverse Displacement, \bar{w} , for [90] Laminate, $S=100$.

S	\bar{w}	Exact (Ren)	CST
2	.803	.999	.0764
4	.278	.312	.0752
10	.108	.115	.0749
50	.0762	.0770	.0748
100	.0751	.0755	.0748
500	.0746	.0749	.0748

TABLE 2. Transverse Displacement, \bar{w} , for Various Shell Thicknesses, [90] Laminate. Classical Solution (CST) taken from [59].

S	$\bar{\sigma}_2$		Exact (Ren)	
	h/2	-h/2	h/2	-h/2
2	-2.52	1.336	-2.455	1.907
4	-1.219	.950	-1.331	1.079
10	-.839	.773	-.890	.807
50	-.761	.744	-.767	.752
100	-.759	.742	-.758	.751
500	-.777	.718	-.752	.750

TABLE 3. Circumferential Stress, $\bar{\sigma}_2$, for Various Shell Thicknesses, [90] Laminate, for $\zeta=h/2$ (bottom) and $\zeta=-h/2$ (top).

S	$\bar{\sigma}_1$		Exact (Ren)	
	h/2	-h/2	h/2	-h/2
2	-.0252	.01336	-.0245	.0816
4	-.0122	.00950	-.0133	.0260
10	-.00839	.00773	-.0089	.0105
50	-.00761	.00744	-.0077	.0076
100	-.00759	.00740	-.0076	.0075
500	-.00777	.00718	-.0075	.0075

TABLE 4. Longitudinal Stress, $\bar{\sigma}_1$, for Various Shell Thicknesses, [90] Laminate, for $\zeta=h/2$ (bottom) and $\zeta=-h/2$ (top).

S	$\bar{\sigma}_4$	Exact (Ren)
2	.489	.555
	* .489	
4	.543	.572
	* .543	
10	.558	.579
	* .559	
50	.528	.568
	* .557	
100	.449	.565
	* .543	
500	.131	.563
	* .314	

TABLE 5. Transverse Shear Stress, $\bar{\sigma}_4$, for Various Shell Thicknesses, [90] Laminate, for $\zeta=0$. Values with an Asterisk Result from Refined 1x20 Mesh.

S	\bar{w}	Exact (Ren)	CST
2	1.141	1.436	.0799
4	.382	.457	.0781
10	.128	.144	.0777
50	.0796	.0808	.0776
100	.0781	.0787	.0776
500	.0774	.0773	.0776

TABLE 6. Transverse Displacement, \bar{w} , for Various Shell Thicknesses, [90/0/90] Laminate. Classical Solution (CST) taken from [59].

S	$\bar{\sigma}_2$		Exact (Ren)	
	h/2	-h/2	h/2	-h/2
2	-3.163	1.732	-3.467	2.463
4	-1.406	1.117	-1.772	1.367
10	-.889	.829	-.995	.897
50	-.789	.774	.798	.782
100	-.787	.770	-.786	.781
500	-.806	.745	-.780	.768

TABLE 7. Circumferential Stress, $\bar{\sigma}_2$, for Various Shell Thicknesses, [90/0/90] Laminate, for $\zeta=h/2$ (bottom) and $\zeta=-h/2$ (top).

S	$\bar{\sigma}_1$		Exact (Ren)	
	h/2	-h/2	h/2	-h/2
2	-.0316	.0173	-.0347	.0871
4	-.0141	.0117	-.0177	.0293
10	-.00889	.00829	-.0100	.0115
50	-.00787	.00774	-.0080	.0079
100	-.00787	.00770	-.0079	.0078
500	-.00806	.00745	-.0078	.0077

TABLE 8. Longitudinal Stress, $\bar{\sigma}_1$, for Various Shell Thicknesses, [90/0/90] Laminate, for $\zeta=h/2$ (bottom) and $\zeta=-h/2$ (top).

S	$\bar{\sigma}_4$	Exact (Ren)
2	.287	.394
	* .287	
4	.326	.476
	* .326	
10	.339	.525
	* .340	
50	.328	.526
	* .340	
100	.291	.523
	* .334	
500	.0853	.525
	* .217	

TABLE 9. Transverse Shear Stress, $\bar{\sigma}_4$, for Various Shell Thicknesses, [90/0/90] Laminate, for $\zeta=0$. Values with an Asterisk result from Refined 1x20 Mesh.

From Table 2, it is evident that by allowing transverse shear deformation in the unidirectional laminate the shell response is much more flexible in the thicker laminates (compare present and exact to the CST solution). For $S=R/h=10$, the present approach underpredicts the transverse displacement, \bar{w} , by 6% yet the classical solution is 35% below the exact result. Similarly, for $S=4$, the present value is 11% below the exact yet the CST solution is 76% less.

For thickness ratios of $S=4$ and lower, we cannot expect close agreement between the present 2-D approach and the exact. Recall that the theory presented in Chapter II clearly uses approximations that invalidate the approach for the very thick geometries. Indeed, for the $S=2$ values shown

in the Tables, the geometry is one of a 3-D solid, certainly not a thin shell (recall earlier assumptions). For these cases the three dimensional effects of nonzero transverse normal stress, σ_3 , and a varying transverse displacement through the thickness, $w(z)$ play a major role in the shell response. Therefore, the entries in all Tables for $S=2$ and to some extent $S=4$ as well, are shown for completeness only, although the majority of the comparisons to the exact values are still quite good.

In Table 2, as the shell becomes very thin for $S=50$ and above, the three approaches converge to the same result as expected since the transverse shear deformation is minimal and classical assumptions are valid. See also Figure 7 for graphical presentation of \bar{w} for $[90]$ laminate.

Similar remarks can be made for the cross ply $[90/0/90]$ laminate, see Table 6 and Figure 8. For $S=10$, the present theory gives the maximum transverse displacement, \bar{w} , 11% below the exact; the classical solution is 46% below the exact. Both 2-D approaches, i.e., present and CST, are in slightly worse agreement compared to the exact than in the unidirectional cases. The previous arguments for the $[90]$ laminate apply to the cross ply laminate in addition to one other comment. The assumed displacements give continuous strains with respect to the transverse coordinate, z . However, discontinuities in stress result due to different constitutive relations in the cross ply laminate for each ply. Although elasticity theory also predicts these

discontinuities only for the inplane stresses, the transverse shear stress, $\bar{\sigma}_4$, must be continuous so that equilibrium is satisfied. The present 2-D approach satisfies equilibrium, generally, only at the midplane of the shell. The consequence of this becomes evident comparing Tables 2 and 6, the transverse displacement response for [90] and [90/0/90] laminates. Further consequences are found by examining the stress results.

Tables 3 and 7 show the results for the circumferential stress, $\bar{\sigma}_2$ for both laminate types. As shown, this stress is calculated very well for both the unidirectional and cross ply laminates even for the thick cases. Recall that the stresses shown for the present case are found at the outermost gauss points within each element. These points do not correspond exactly to the center of laminate as the Table indicates. Increased accuracy in $\bar{\sigma}_2$ could be attained by a mesh refinement near the center of the shell thereby moving the gauss points closer to the actual shell center or by extrapolating the stresses to give nodal values.

Improving the numerical aspects of the solution as just described will increase the accuracy somewhat for the thicker shell geometries as well. However, the largest loss of accuracy for these cases is due to the 2-D assumption of the present approach, i.e., neglect of σ_3 in the solution. Notice in Tables 3 and 7 that the present results are the most inaccurate at the top of the shell, i.e., where the load is applied, and therefore, where the effects of σ_3 are

generally the most significant. The circumferential stress, $\bar{\sigma}_2$, is also plotted as a function of thickness in Figures 9-12.

Tables 4 and 8 give the longitudinal stresses, $\bar{\sigma}_1$, in the shell. The comparisons for both laminate types to the exact are fairly good except for thicknesses of $S=4$ and thicker. In the very thick cases, the longitudinal stress is significantly underestimated on the top surface of the shell, i.e., at $\zeta=-h/2$. Apparently, the influence of the three dimensionality, i.e., σ_3 on the top of the shell where loading acts, has a great effect for this stress. The influence is much less at the bottom of the shell where σ_3 is identically zero, see [59].

The transverse shear stress, $\bar{\sigma}_4$, is calculated at the midplane of the unidirectional laminate very well for values as small as $S=4$, see Table 5. The stress for $S=500$ as predicted in the present approach is inaccurate because its gradient is so high for this thickness near the support. A more accurate value should be attainable if a further refined mesh were analyzed and therefore, the gauss point where $\bar{\sigma}_4$ is calculated would be closer to the end support. Figures 13-15 show the transverse shear stress as a function of thickness for the unidirectional case. Notice that as the laminate becomes thicker, the exact transverse shear stress becomes more asymmetrical, whereas the present approach always gives a symmetric response about the midplane. Recall that the cubic term in the stress

expression for the present approach which gives this asymmetry was neglected as small, see text following Eqn (16). The Figures show that this is a good assumption since the asymmetry is significant only for the thick $S=4$ case.

Similarly, the transverse stress, $\bar{\sigma}_4$, is given for the cross ply laminate in Table 9 and in Figures 16-18. As argued previously, the discontinuities in $\bar{\sigma}_4$ as a function of transverse coordinate, ζ , violate equilibrium away from the shell midplane and thus explains the disagreement shown. Notice that the results from the present theory at the ply interfaces are approximately equidistant from the exact value at the interfaces.

Finally, Figures 19 and 20 show the circumferential displacement, \bar{v} , taken at the left support for both laminate types. The present approach, with an assumed cubic function through the thickness, slightly underestimates the exact values and but captures the distribution very well. At the midplane where $\bar{\sigma}_4$ is typically maximum, the shear deformable theories give a slightly steeper slope compared to the CST result and gradually approach the same slope at the outer ζ coordinates of the shell where the shear deformation is zero.

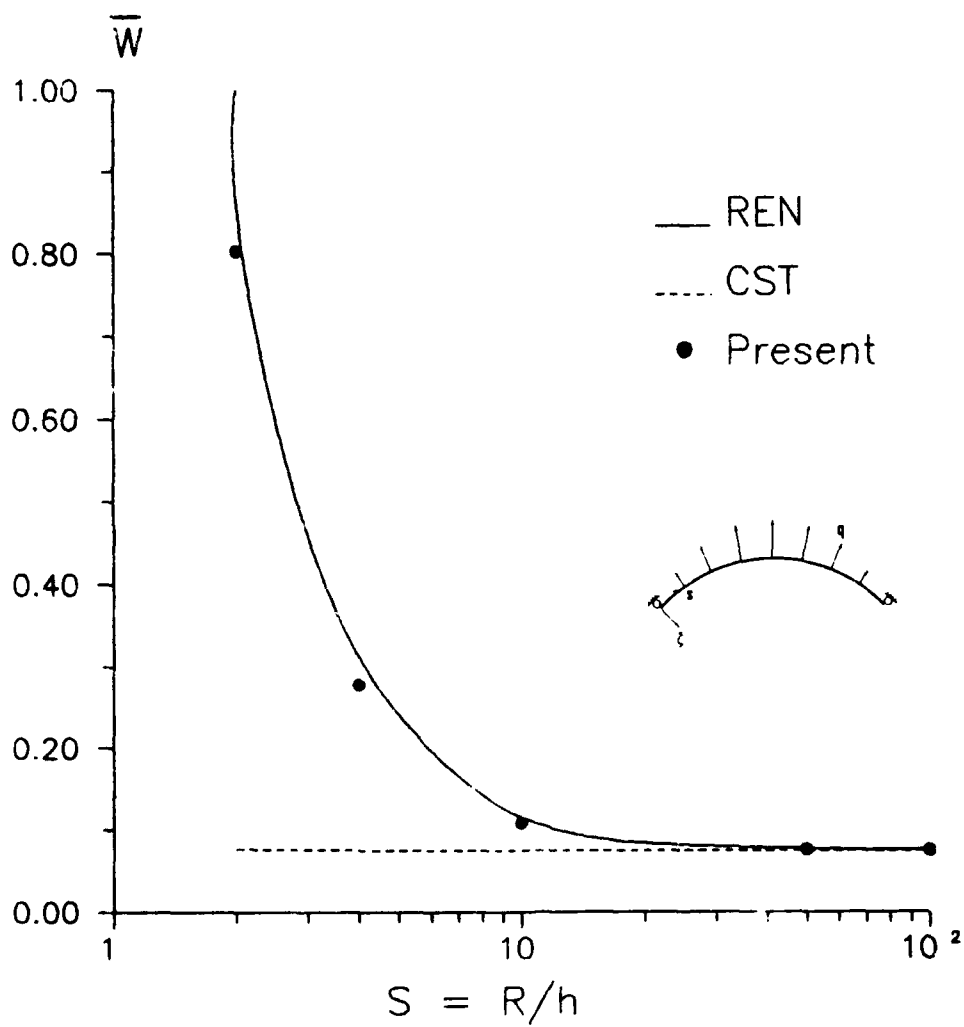


FIGURE 7. Transverse Displacement, \bar{w} , versus Shell Thickness, S , for [90] Laminate.

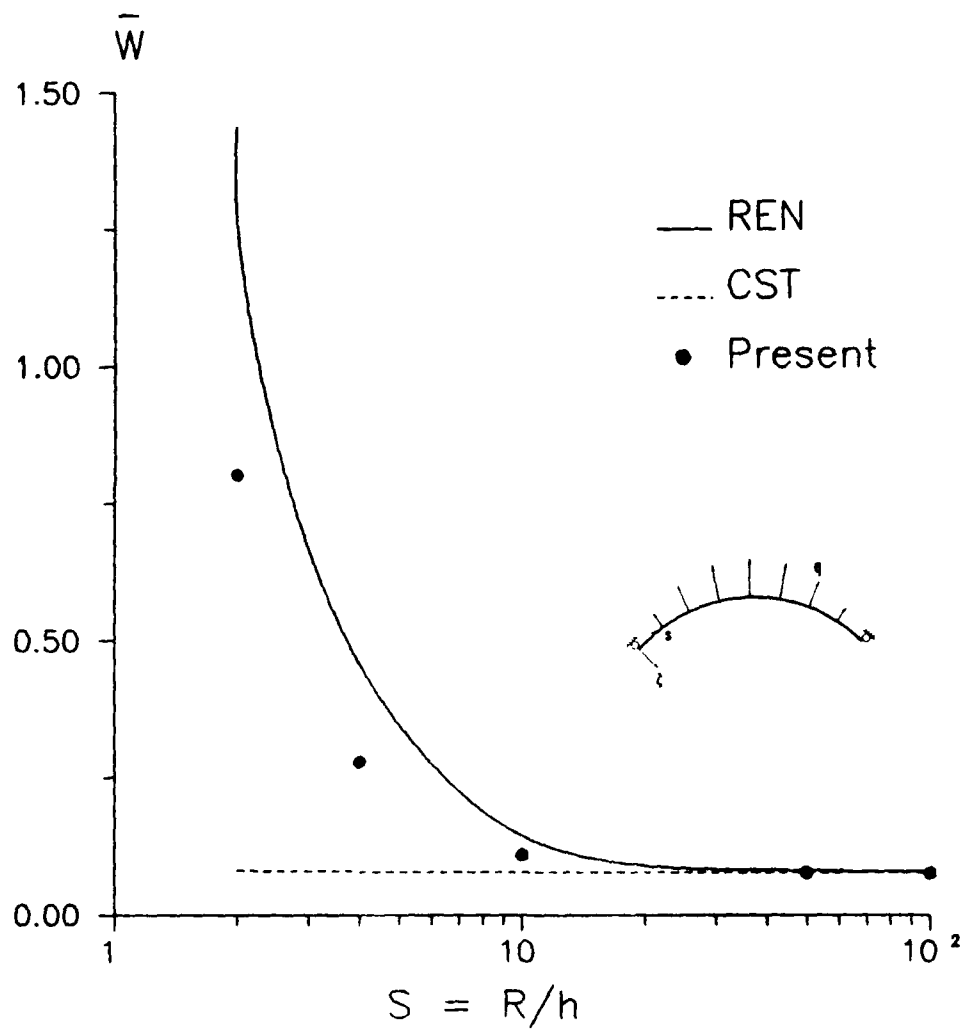


FIGURE 8. Transverse Displacement, \bar{w} , versus Shell Thickness, S , for [90/0/90] Laminate.

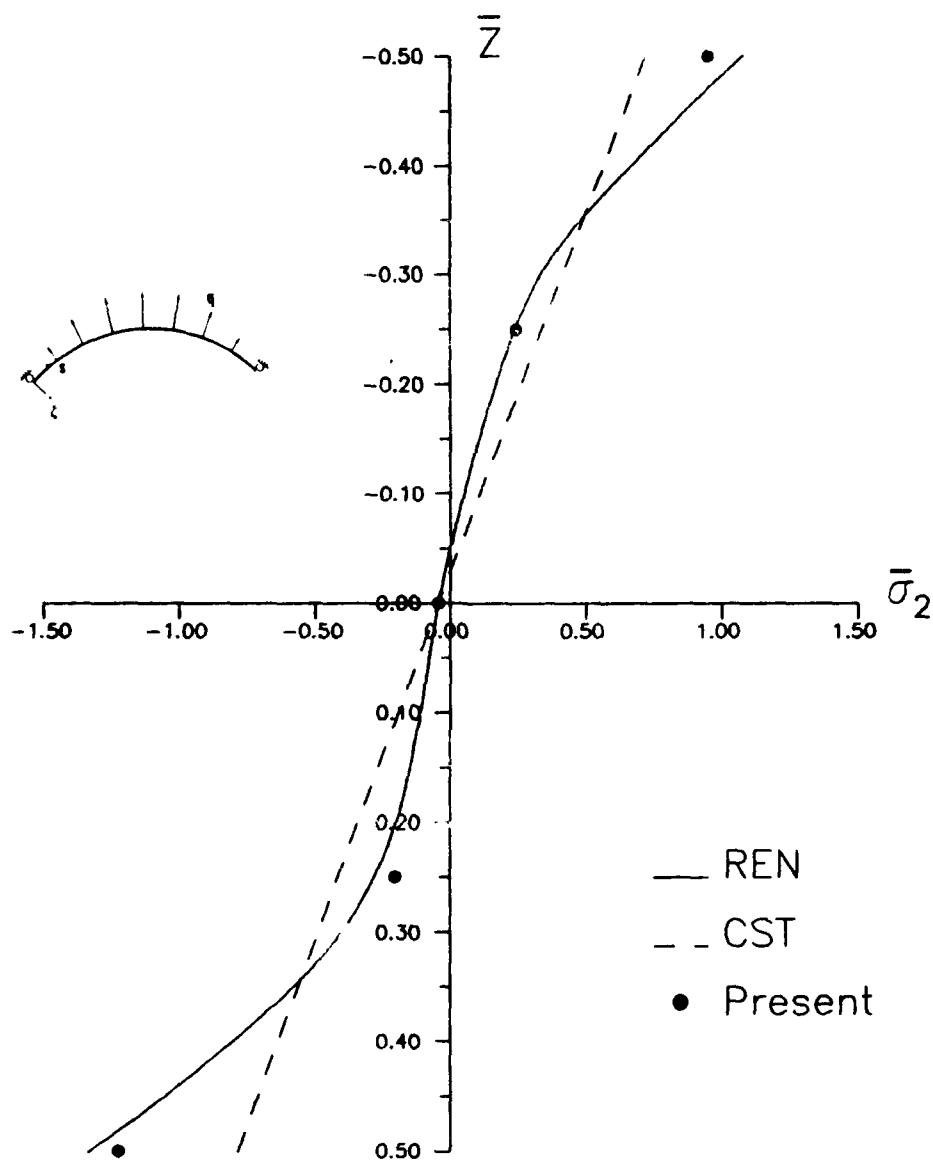


FIGURE 9. Circumferential Stress, $\bar{\sigma}_2$, Through the Thickness for S=4, [90] Laminate.

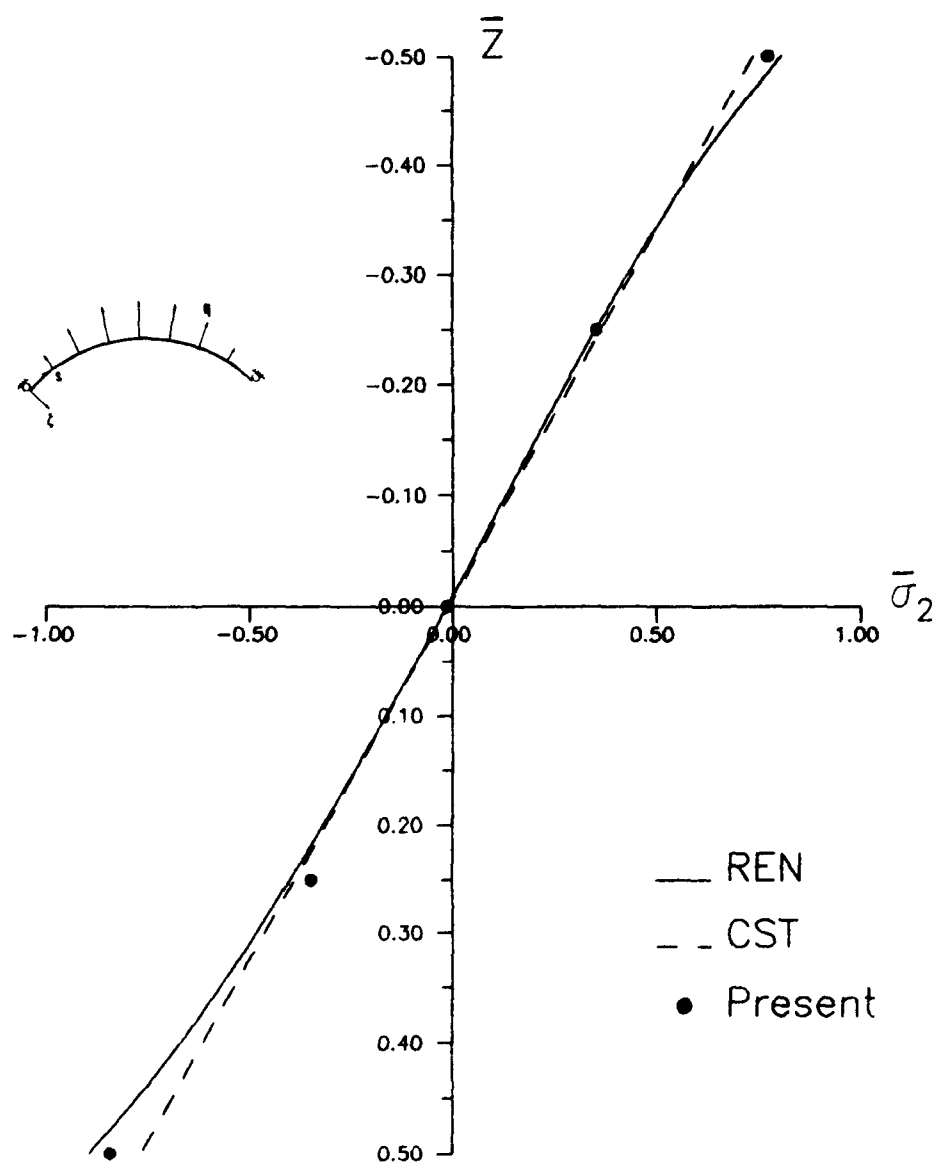


FIGURE 10. Circumferential Stress, $\bar{\sigma}_2$, Through the Thickness for $S=10$, [90] Laminate.

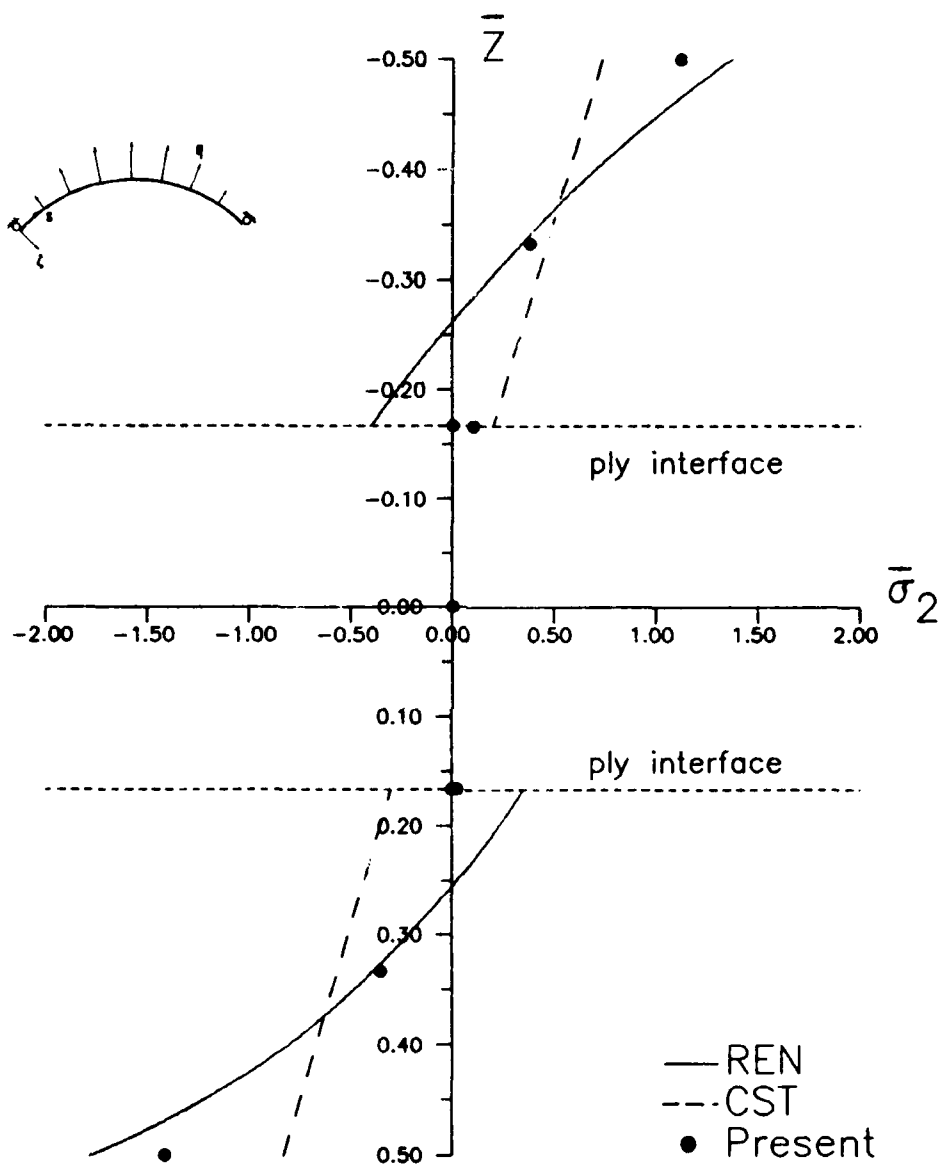


FIGURE 11. Circumferential Stress, $\bar{\sigma}_2$, Through the Thickness for $S=4$, $[90/0/90]$ Laminate.

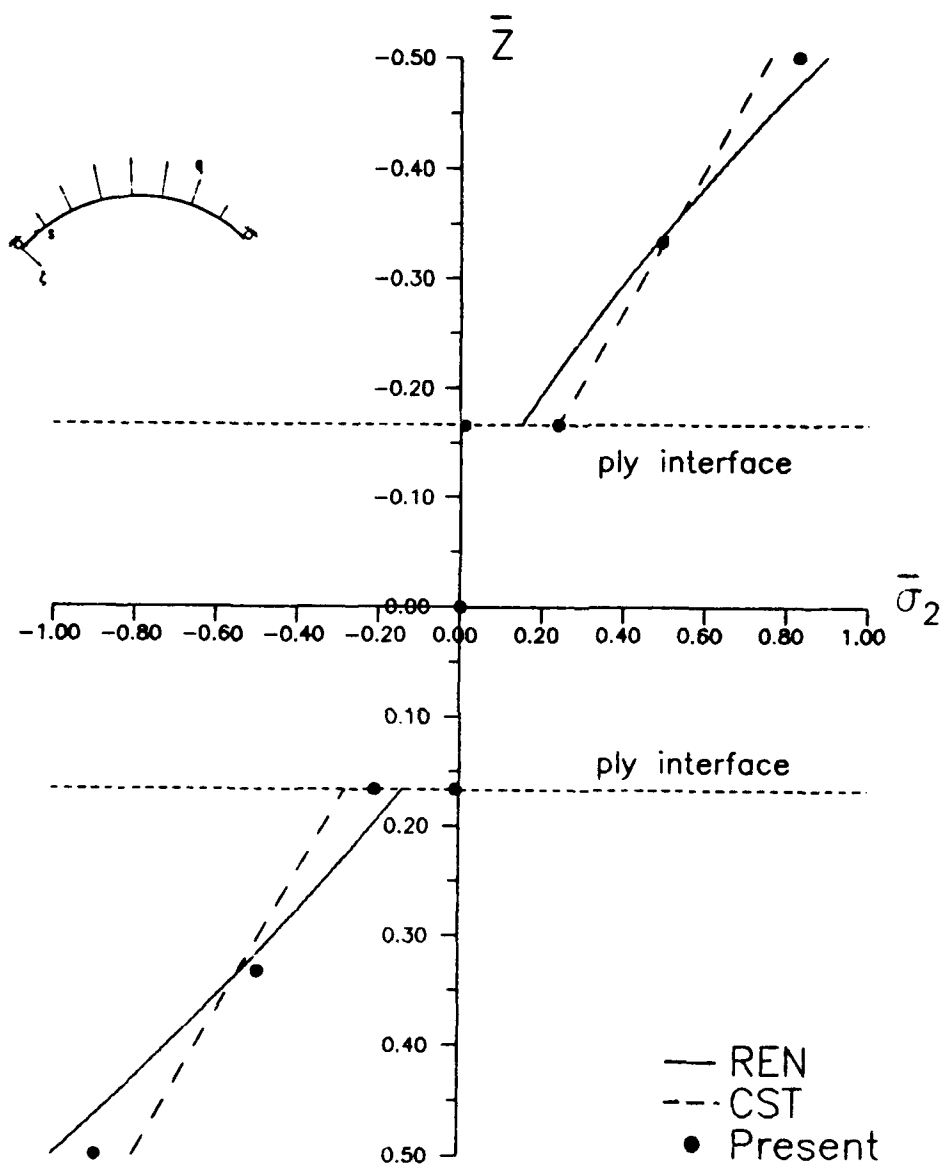


FIGURE 12. Circumferential Stress, $\bar{\sigma}_2$, Through the Thickness for $S=10$, [90/0/90] Laminate.

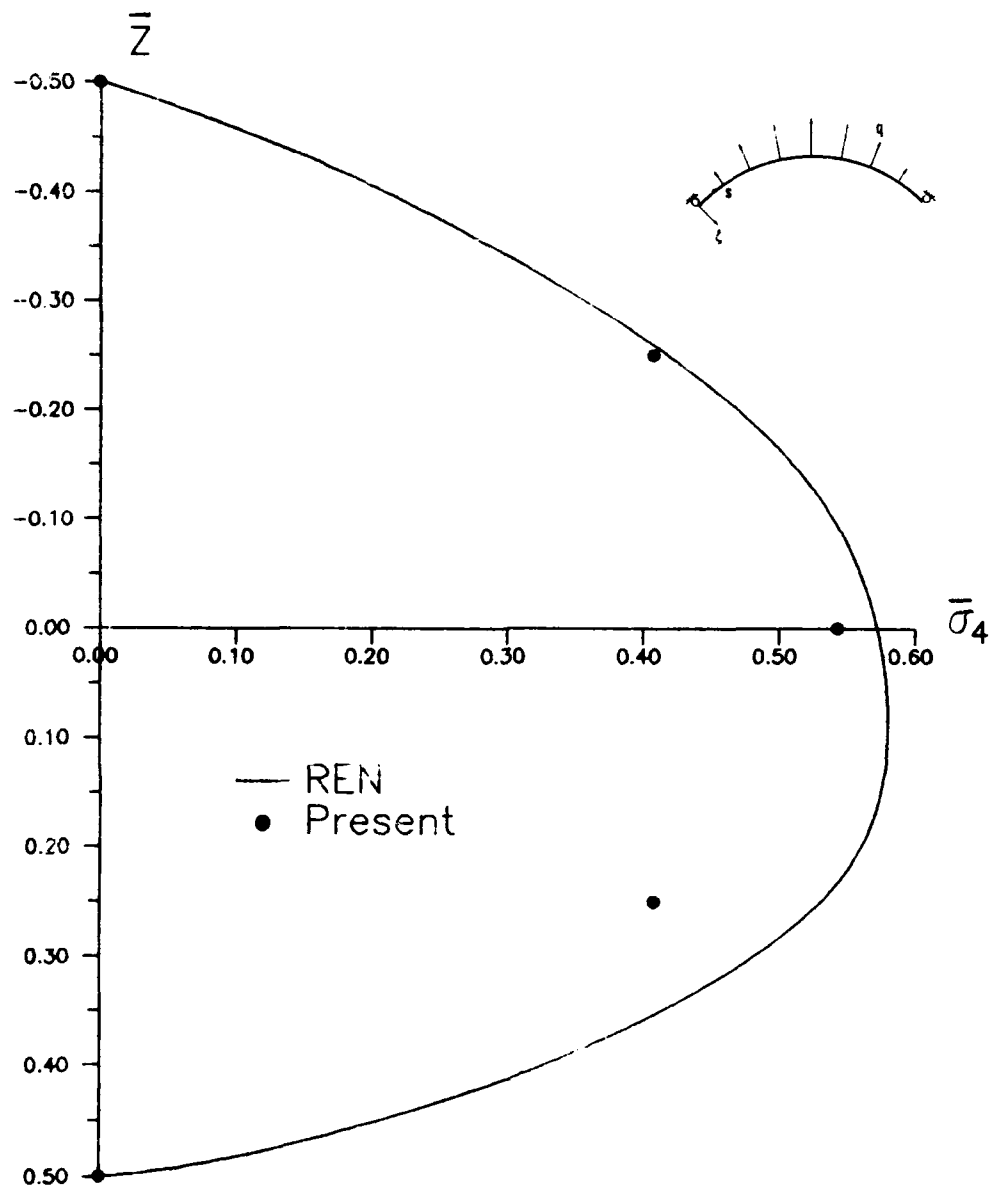


FIGURE 13. Transverse Shear Stress, $\bar{\sigma}_4$, Through the Thickness for $S=4$, $[90]$ Laminate.

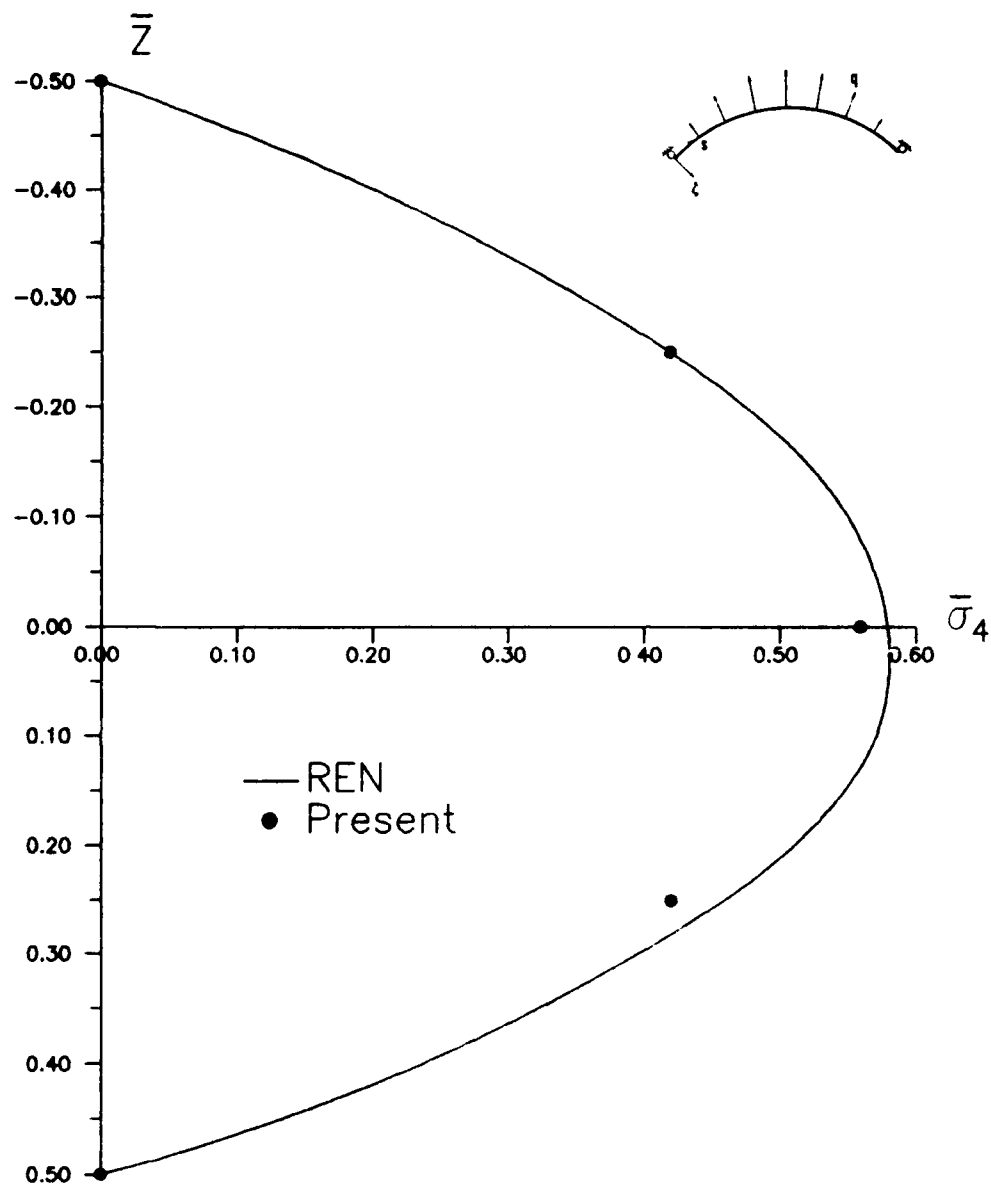


FIGURE 14. Transverse Shear Stress, $\bar{\sigma}_4$, Through the Thickness for $S=10$, $[90]$ Laminate.

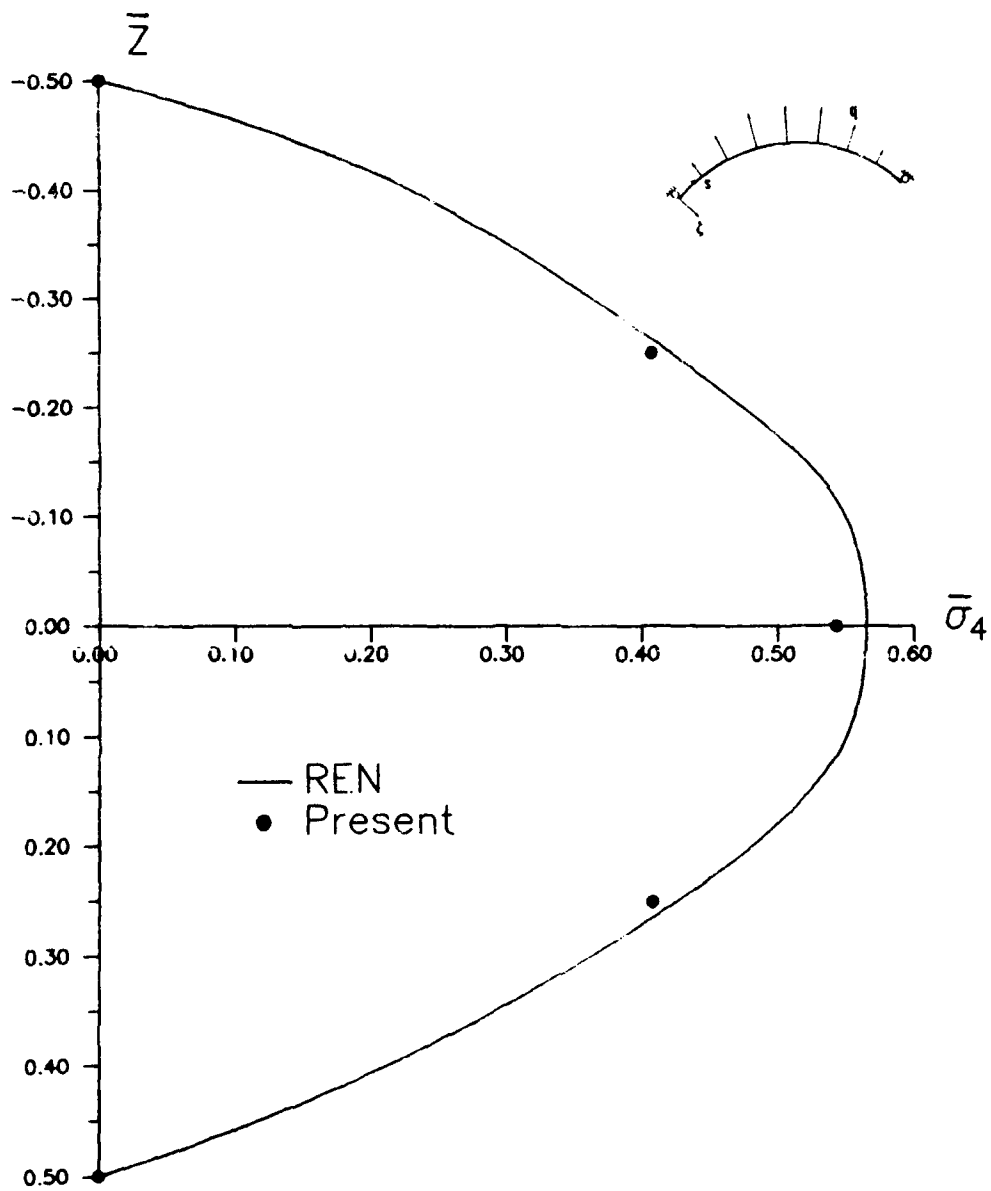


FIGURE 15. Transverse Shear Stress, $\bar{\sigma}_4$, Through the Thickness for $S=100$, $[90]$ Laminate.

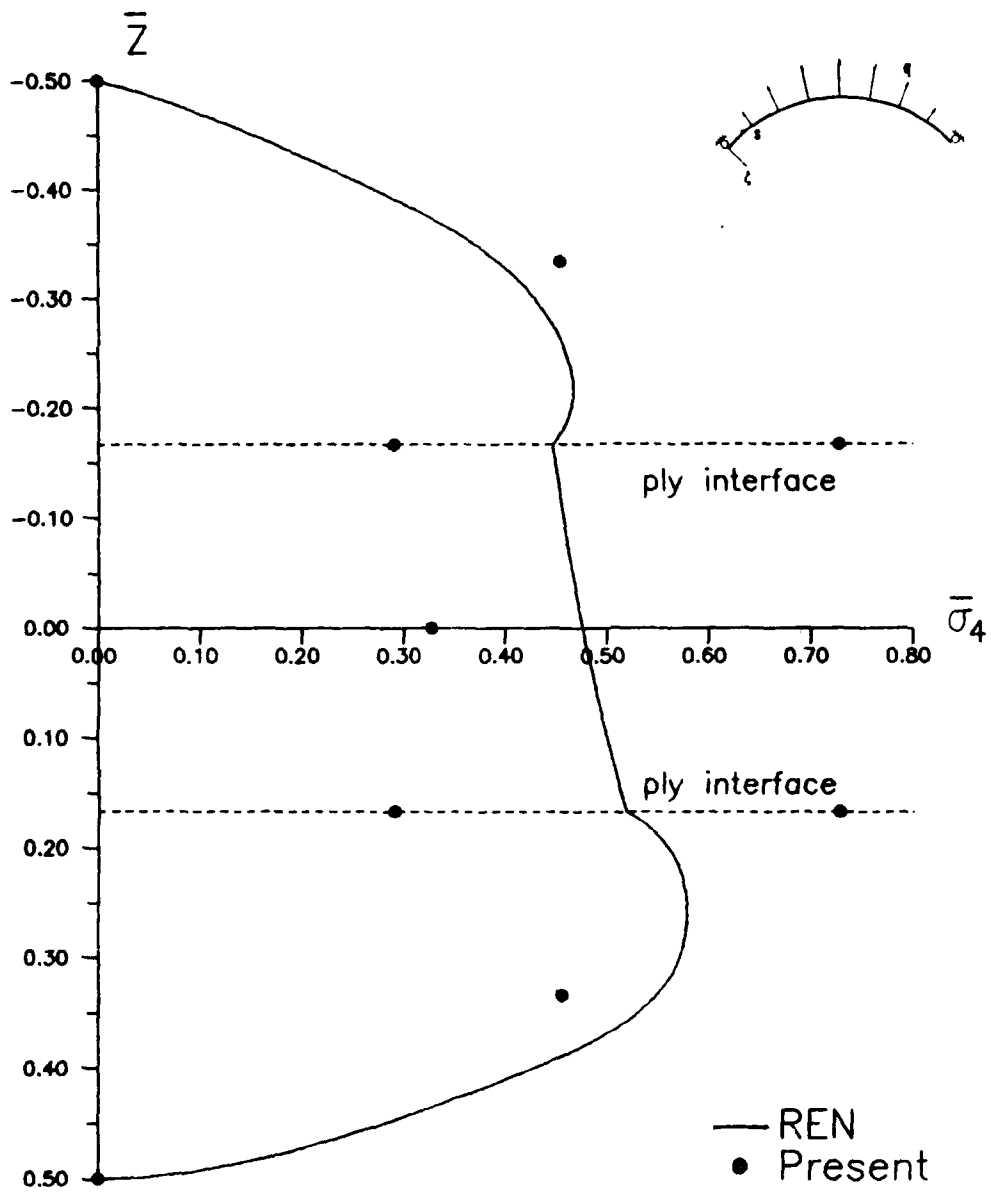


FIGURE 16. Transverse Shear Stress, $\bar{\sigma}_4$, Through the Thickness for S=4, [90/0/90] Laminate.

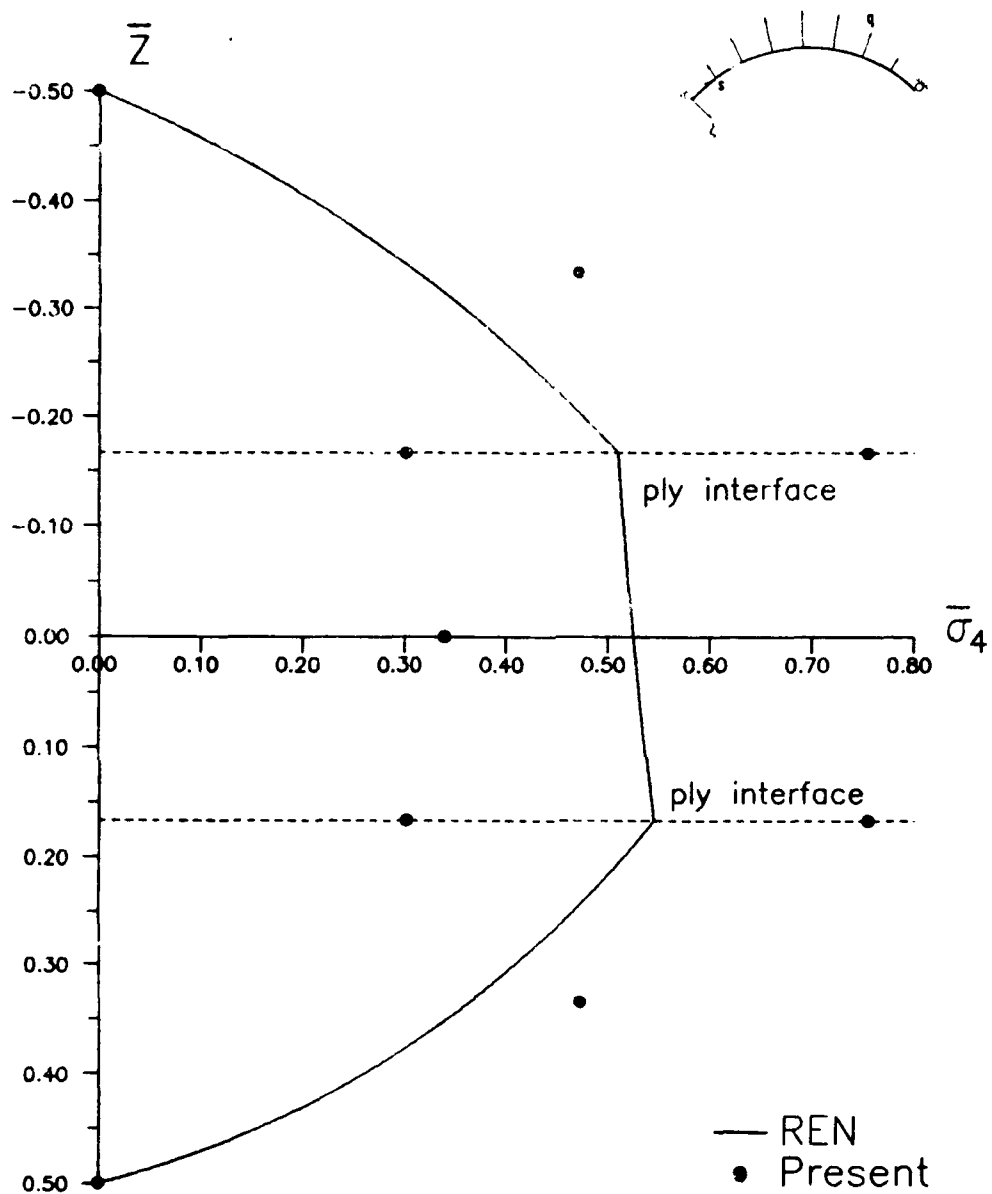


FIGURE 17. Transverse Shear Stress, $\bar{\sigma}_4$, Through the Thickness for $S=10$, $[90/0/90]$ Laminate.

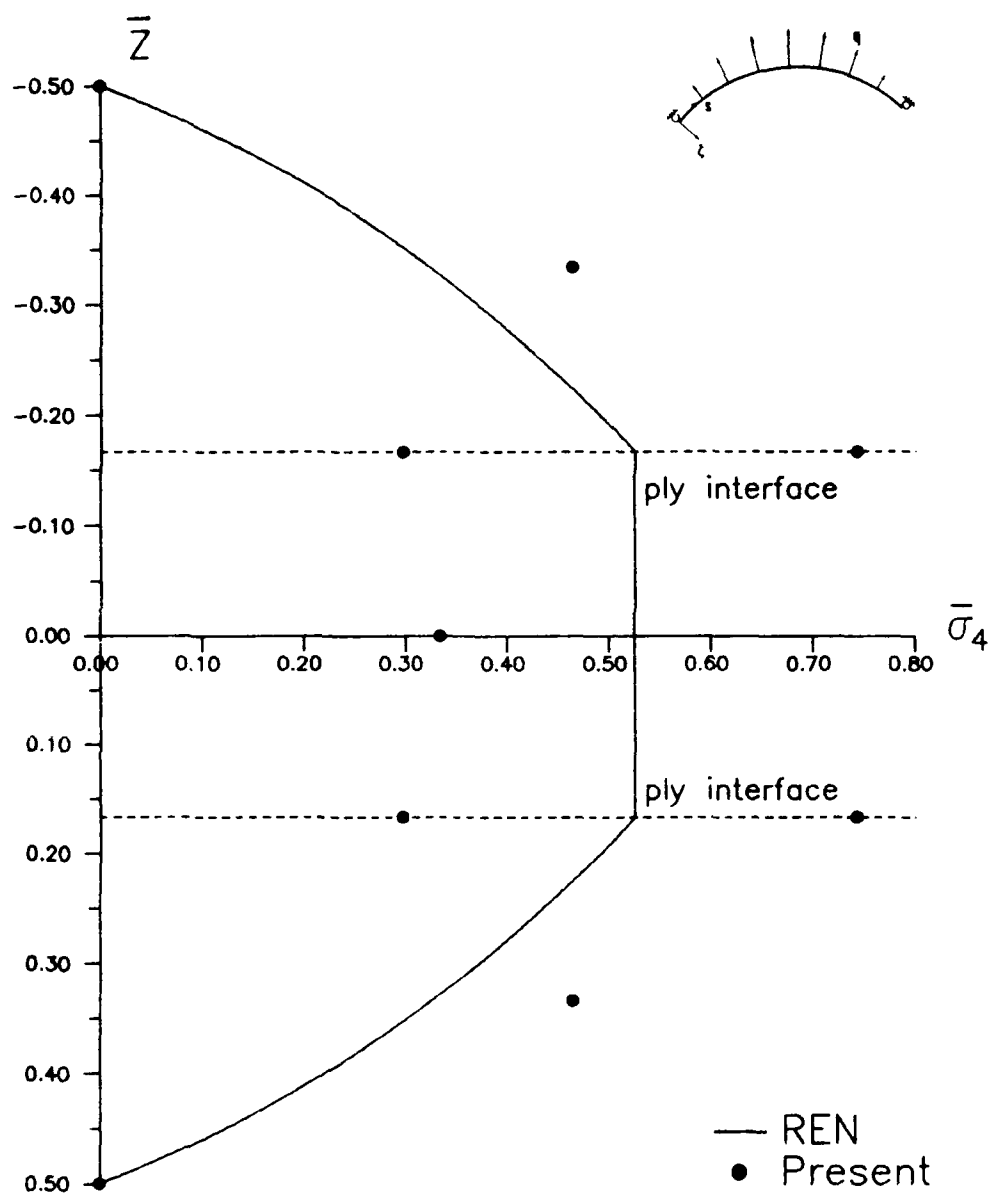


FIGURE 18. Transverse Shear Stress, $\bar{\sigma}_4$, Through the Thickness for $S=100$, $[90/0/90]$ Laminate.

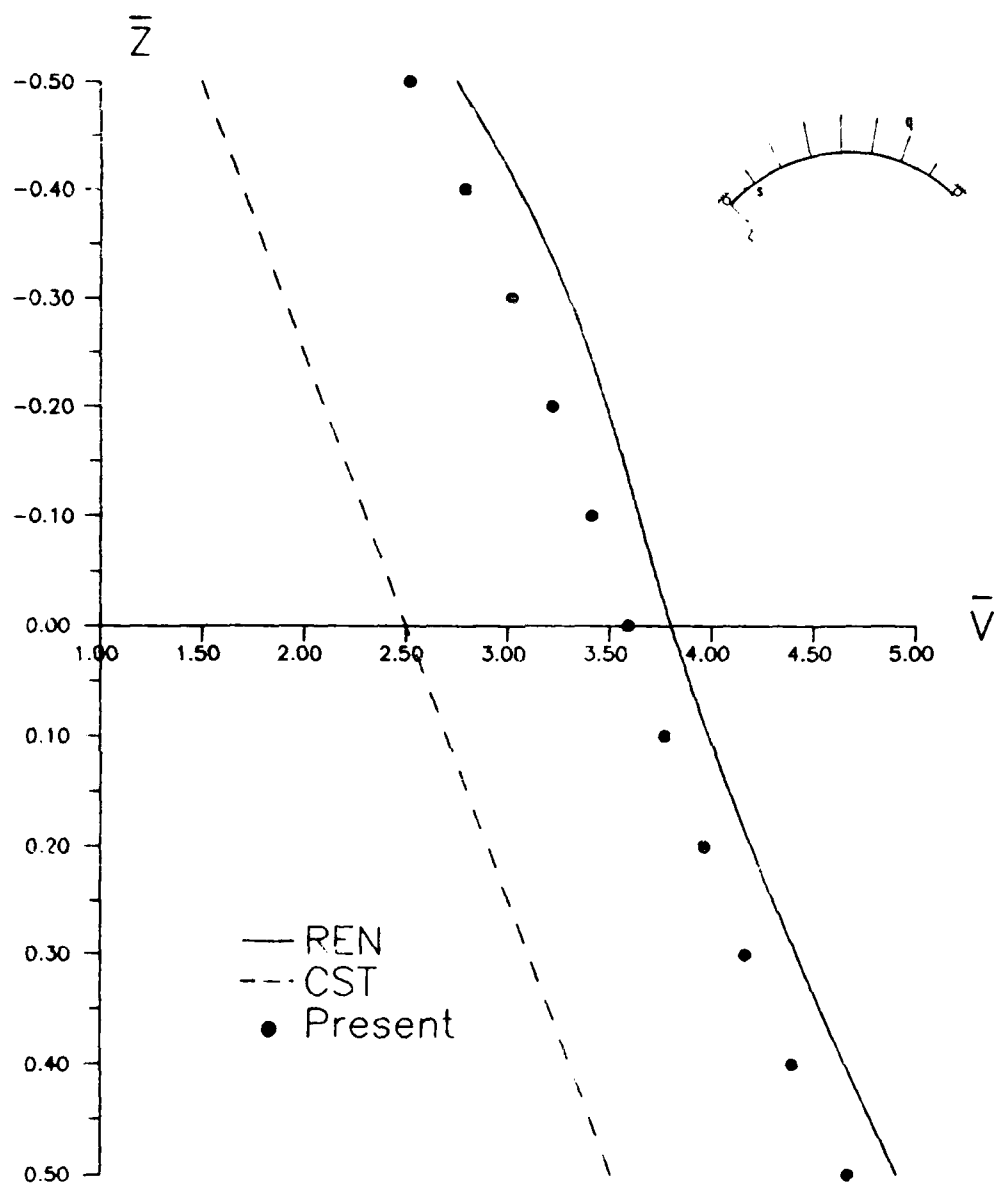


FIGURE 19. Circumferential Displacement, \bar{V} , Through the Thickness for $S=10$, $[90]$ Laminate.

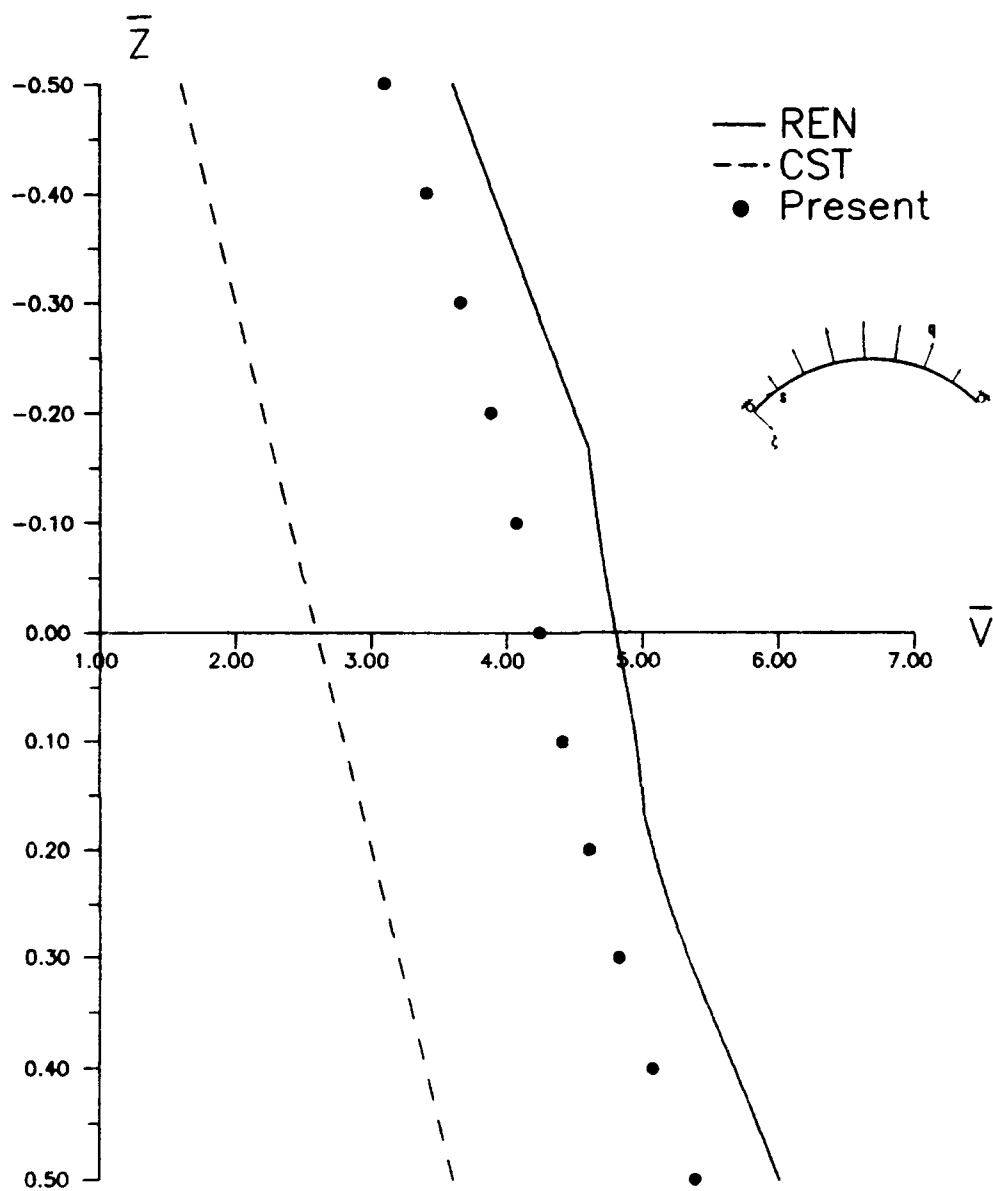


FIGURE 20 Circumferential Displacement, \bar{V} , Through the Thickness for $S=10$, $[90/0/90]$ Laminate.

V. Conclusions

A higher order shell finite element theory has been developed that includes a through the thickness parabolic shear stress distribution. The element has 36 degrees of freedom and avoids the locking phenomenon usually associated with shell elements. Laminated composite construction can be considered. Exact Green strain relations are included so that large displacement, simplified large rotation (up to the assumption of linear strain displacement relations for the transverse strains) degrees of freedom can be investigated. The approach is applied to a laminated cylindrical shell in cylindrical bending and linear results are compared to the exact elasticity solution. Displacements and stresses are predicted very well for the unidirectional laminate even for very thick geometries. Stresses are predicted less accurately for the cross ply laminate due to violation of equilibrium away from the midplane of the shell, a consequence of the 2-D approach.

Bibliography

1. Saada, A.S. Elasticity Theory and Applications, Pergamon Press, (1974).
2. Marlowe, M.B. and W. Flugge. Some New Developments in the Foundations of Shell Theory, LSMC-6-78-68-13, (1968).
3. Mollman, H. Introduction to the Theory of Thin Shells, John Wiley and Sons, (1981).
4. Niordson, F.I. Introduction To Shell Theory, Technical University of Denmark, (1980).
5. Dong, S.B., K.S. Pister, and R.L. Taylor. "On the Theory of Laminated Anisotropic Shells and Plates," J Aeronaut Sci, 29, (1962).
6. Bert, C.W. "Structural Theory for Laminated Anisotropic Elastic Shells," Jnl Compos Mater, 1, (1967).
7. Bogner, F.K., R.L. Fox, and L.A. Schmit. "A Cylindrical Shell Discrete Element," AIAA J, 5, 4, (1967).
8. Yang, T.Y. "High Order Rectangular Shallow Shell Finite Element," J Engng Mech Div, ASCE EMI, (1973).
9. Cheng, S. and F.B. He. "Theory of Orthotropic and Composite Cylindrical Shells, Accurate and Simple Fourth Order Governing Equations," J Appl Mech, 51, (1984).
10. Koiter, W.T. "A Consistent First Approximation in the General Theory of Thin Elastic Shells," Proc Sym on Theory of Thin Elastic Shells, Amsterdam, North Holland, (1960).
11. Hildebrand, F.B., E. Reissner, and G.B. Thomas. Notes on the Foundations of the Theory of Small Displacements of Orthotropic Shells, NACA-TN-1833, (1949).
12. Naghdi, P.M. "On the Theory of Thin Elastic Shells," Q Appl Math, 14, (1957).
13. Reissner, E. "The Effect of Transverse Shear Deformation on the Bending of Elastic Plates," J Appl Mech, (1945).
14. Reissner, E. Small Bending and Stretching of Sandwich Type Shells, NACA-TN-1832, (1949).
15. Mindlin, R.D. "Influence of Rotatory Inertia and Shear on Flexural Motions of Isotropic Elastic Plates," J Appl Mech, 18, (1951).

16. Yang, Morris, and Stavsky. "Elastic Wave Propagation in Heterogeneous Plates," Int J Solids & Struct, 2, (1966).
17. Whitney, J.M. and M.J. Pagano. "Shear Deformation in Heterogeneous Plates," J Appl Mech, (1970).
18. Reddy, J.N. "Exact Solutions of Moderately Thick Laminated Shells," J Engng Mech Div, ASCE 110, 5, (1984).
19. Noor, A.K. "Stability of Multilayered Composite Plates," Fibre Science and Tech, 8, (1975).
20. Reddy, J.N. and W.C. Chao. "A Comparison of Closed Form and Finite Element Solution of Thick Laminated Anisotropic Rectangular Plates," Nucl Eng & Des, 64, (1981).
21. Noor, A. and M.D. Mathers. Shear Flexible Finite Element Models of Laminated Composite Plates and Shells, NASA TN D8044, (1975).
22. Ahmad, S., B. Irons, and O.C. Zienkiewicz. "Analysis of Thick and Thin Shell Structures by Curved Finite Elements," IJNME, 2, (1970).
23. Zienkiewicz, O.C., R.D. Taylor, and J.M. Too. "Reduced Integration Technique in General Analysis of Plates and Shells," IJNME, 3, (1971).
24. Kui, L.X., G.Q. Liu, and O.C. Zienkiewicz. "A Generalized Method for the Finite Element Analysis of Thin Shells," IJNME, 21, (1985).
25. Levinson, M. "An Accurate Simple Theory of the Statics and Dynamics of Elastic Plates," Mech Research Comm, 7, (1980).
26. Murthy, M.V.V. An Improved Transverse Shear Deformation Theory for Laminated Anisotropic Plates, NASA-TP-1903, (1981).
27. Reddy, J.N. "A Simple Higher Order Theory for Laminated Composite Plates," J Appl Mech, 51, (1984).
28. Reddy, J.N. and N.D. Phan. "Stability and Vibration of Isotropic, Orthotropic, and Laminated Plates According to a Higher Order Shear Deformation Theory," J Sound & Vib, 98(2), (1985).
29. Phan, N.D. and J.N. Reddy. "Analysis of Laminated Composite Plates Using a Higher Order Shear Deformation Theory," IJNME, 21, (1985).

30. Reddy, J.N. and C.F. Liu. "A Higher Order Shear Deformation Theory of Laminated Elastic Shells," Int J Eng Sci. 23,3, (1985).
31. Bhimaraddi, A. "A Higher Order Theory for Free Vibration Analysis of Circular Cylindrical Shells," Int J Solids & Struct. 20, 7, (1984).
32. Bhimaraddi, A. "Generalized Analysis of Shear Deformable Rings and Curved Beams", Int Solids & Struct. 24, 7, (1988).
33. Soldatos, K.P. "Buckling of Axially Compressed Antisymmetric Angle Ply Laminated Circular Cylindrical Panels According to a Refined Shear Deformable Shell Theory," PVP, 116, (1987).
34. Soldatos, K.P. "Stability and Vibration of Thickness Shear Deformable Cross-Ply Laminated Non-Circular Cylindrical Shells," PVP, 115, ASME, (1986).
35. Brush, D.O. and B.O. Almroth. Buckling of Bars, Plates, and Shells, McGraw Hill, (1975).
36. Novozhilov, V.V. Foundations of the Nonlinear Theory of Elasticity, Graylock Press, (1953).
37. Librescu, L. and R. Schmidt. "Refined Theories of Elastic Anisotropic Shells Accounting for Small Strains and Moderate Rotations," Int J. Non-linear Mechanics, , (1988).
38. Sanders, J.L. "Nonlinear Theories for Thin Shells," Appl Math., XXI(1), (1962).
39. Librescu, L. "Refined Geometrically Nonlinear Theories of Anisotropic Laminated Shells", Q Appl Math. 45, (1987).
40. Schmit, L.A. and B.R. Monforton. "Finite Deflection Discrete Element Analysis of Sandwich Plates and Cylindrical Shells with Laminated Faces," AIAA J. 8, 8, (1970).
41. Stolarski, H., T.Belyschko, N. Carpenter, and J. Kennedy. "A Simple Triangular Curved Shell Element for Collapse Analysis," in Collapse Analysis of Structures, ed by L.H. Sobel and K Thomas, PVP, 84, ASME, (1984).
42. Reddy, J.N. and K. Chandrashekhara. "Nonlinear Analysis of Laminated Shells including Transverse Shear Strains," AIAA J., 23, 3, (1985).
43. Reddy, J.N. "Geometrically Nonlinear Transient Analysis of Laminate Composite Plates," AIAA J. 21,4 (1983).

44. Putcha, N.S. and J.N. Reddy. "A Refined Mixed Shear Flexible Finite Element for the Nonlinear Analysis of Laminated Plates," Comp and Struct, 22, 4, (1986).
45. Noor, A. and J. Peters. "Nonlinear Analysis of Anisotropic Panels," AIAA J, 24, 9, (1986).
46. Meroueh, K.A. "On a Formulation of a Nonlinear Theory of Plates and Shells with Applications," Comp and Struct, 24, 5, (1986).
47. Surana, K.S. "Geometrically Nonlinear Formulation for Curved Shell Elements," IJNME, 19, (1983).
48. Surana, K.S. "A Generalized Geometrically Nonlinear Formulation with Large Rotations for Finite Elements with Rotational Degrees of Freedom," Comp and Struct, 24, (1986).
49. Stein, M. "Nonlinear Theory for Plates and Shells Including the Effects of Transverse Shearing," AIAA J, 24, 9, (1986).
50. Palazotto, A.N. and W.P. Witt. "Formulation of a Nonlinear Compatible Finite Element for Analysis of Laminated Composites," Comp and Struct, 21, 6, (1985).
51. Hinrichsen, R.L. and A.N. Palazotto. "Nonlinear Finite Element Analysis of Thick Composite Plates Using a Cubic Spline Function," AIAA J, 24, 11, (1986).
52. Bathe, K.J. Finite Element Procedures in Engineering Analysis, Prentice Hall, (1982).
53. Washizu, K. Variational Methods in Elasticity and Plasticity, Pergamon Press, (1982).
54. Dennis, S.T. and A.N. Palazotto. "Transverse Shear Deformation in Orthotropic Cylindrical Pressure Vessels Using a Higher Order Shear Theory," AIAA J (to appear)
55. Koiter, W.T. "Foundations and Basic Equations of Shell Theory-A Survey of Recent Progress," IUTAM Symposium, Copenhagen, (1967), in Theory of Thin Shells, ed. by F.I. Niordson.
56. John, F. "Estimates for the Derivatives of the Stresses in a Thin Shell and Interior Shell Equations," Communications on Pure and Appl Math, Vol XVIII, (1965).
57. Pagano, N.J. "Exact Solutions for Composite Laminates in Cylindrical Bending," Jnl Compos Mater, 3, (1969).

58. Pagano, M.J. "Exact Solutions for Rectangular Bidiirectional Composites and Sandwich Plates," Int Compos Mater, 4, (1973).
59. Ren, J.G. "Exact Solutions for Laminated Cylindrical Shells in Cylindrical Bending", Composites Sci Tech, 29, (1987).
60. Tsai, S.W. Composite Design, Rank Composites, (1987).
61. Rajasekaran, S. and D.W. Murray. "Incremental Finite Element Matrices", J Struct Div, ASCE, (1973).
62. Cook, R.D. Concepts and Applications of Finite Element Analysis, John Wiley and Sons, (1981).
63. Waiz, G.E., R.E. Fulton, and M.G. Cyrus. Accuracy and Convergence of Finite Element Approximations, AFFDL-TR-68-150, (1968).
64. Dadeppo D.A. and J. Schmidt. "Instability of Clamped Ring-Circular Arches Subjected to a Point Load," Journ of Appl Mech, 42, (1975).
65. Huddleston J.V. "Finite Deflections and Snap Through of High Circular Arches," Journ of Appl Mech, Dec (1968).
66. Dennis, S.T. Large Displacement and Rotational Formulation for Laminated Shells Including Parabolic Transverse Shear, AFIT/DS/AA/88-1, Air Force Institute of Technology, Wright-Patterson AFB OH (1988).
67. Dennis, S.T. and A.N. Palazotto. "Large Displacement and Rotational Formulation for Laminated Shells Including Parabolic Transverse Shear," Int J Non-Linear Mech (to appear).
68. Noor, A.K. and W.S. Burton. "Assessment of Shear Deformation Theories for Multilayered Composite Plates," Appl Mech Rev, 42, 1, (1989).
69. Kapania, R.K. "A Review on the Analysis of Laminated Shells," Journ of Press Vess Tech, 111, (1989).
70. Schmidt, R. and J.W. Reddy. "A Refined Small Strain and Moderate Rotation Theory of Elastic Anisotropic Shells", Journ of Appl Mech, Sep (1988).
71. Pietraszkiewicz, W. "Lagrangian Description and Incremental Formulation of the Nonlinear Theory of Thin Shells," Int J Non-Linear Mech, 19, 2, (1983).

Appendix

(A1)

note: cylindrical coordinates, i.e., $\alpha_\gamma=1$, $R_1=\infty$, $c=1/R_2=1/R$.

$$\varepsilon_1 = \varepsilon_1^0 + \zeta^p \kappa_{1p}. \quad (A2)$$

$$\varepsilon_1^0 = u_{,1} + 1/2(u_{,1}^2 + v_{,1}^2 + w_{,1}^2) \quad (a)$$

$$\kappa_{11} = \psi_{1,1} - v_{,1}^2 c^2 + \psi_{1,1} u_{,1} + \psi_{2,1} v_{,1} \quad (b)$$

$$\kappa_{12} = v_{,1}^2 c^2 / 2 - \psi_{2,1} v_{,1} c + 1/2(\psi_{1,1}^2 + \psi_{2,1}^2) \quad (c)$$

$$\kappa_{13} = k(w_{,11} + \psi_{1,1}) + u_{,1} k(w_{,11} + \psi_{1,1}) + v_{,1} k(w_{,21} + \psi_{2,1}) \quad (d)$$

$$\begin{aligned} \kappa_{14} = & -v_{,1} k c (w_{,21} + \psi_{2,1}) + \psi_{1,1} k (w_{,11} + \psi_{1,1}) \\ & + \psi_{2,1} k (w_{,21} + \psi_{2,1}) \end{aligned} \quad (e)$$

$$\kappa_{15} = 0 \quad (f)$$

$$\begin{aligned} \kappa_{16} = & (k/2)^2 (w_{,11}^2 + 2w_{,11}\psi_{1,1} + \psi_{1,1}^2 + w_{,21}^2 \\ & + 2w_{,21}\psi_{2,1} + \psi_{2,1}^2) \end{aligned} \quad (g)$$

$$\kappa_{17} = 0 \quad (h)$$

$$\varepsilon_2 = \varepsilon_2^0 + \zeta^P \kappa_{2P}, \quad (A3)$$

$$\varepsilon_2^0 = \psi_{2,2} - wc + 1/2(v_{2,2}^2 + w_{2,2}^2 + u_{2,2}^2 - v_2^2 c^2 + u_2^2 c^2) + w_{2,2}c - v_{2,2}wc \quad (a)$$

$$\kappa_{21} = \psi_{2,2} - wc^2 + u_{2,2}^2 c + w_{2,2}^2 c + w_{2,2}^2 c - 2(v_{2,2}w_{2,2} + v_2 w_{2,2} + v_2 w_{2,2}^2 + v_{2,2}^2 w_{2,2} + v_{2,2}^2 w_{2,2}^2 - c(\psi_{2,2}w_{2,2} - w_{2,2}w_{2,2})) \quad (b)$$

$$\kappa_{22} = \psi_{2,2}c + 1/2(v_{2,2}^2 + w_{2,2}^2 + u_{2,2}^2 - v_2^2 c^2 + u_2^2 c^2) + v_2 w_{2,2}^2 - 2c^2(\psi_{2,2}w_{2,2} - w_{2,2}w_{2,2}) + \psi_{2,2}v_{2,2}c \quad (c)$$

$$\kappa_{23} = k(w_{2,2} + \psi_{2,2}) + c(\psi_{2,2}^2 + \psi_{1,2}^2) + ku_{2,2}(w_{1,2} + \psi_{1,2}) + \psi_{2,2}^2 c^3 + kv_{2,2}(w_{2,2} + \psi_{2,2}) + vkc^2(w_{2,2} + \psi_{2,2}) - wkc(w_{2,2} + \psi_{2,2}) + w_{2,2}kc(w_{2,2} + \psi_{2,2}) \quad (d)$$

$$\kappa_{24} = kc(w_{2,2} + \psi_{2,2}) + 2u_{2,2}kc(w_{1,2} + \psi_{1,2}) + vkc^3(w_{2,2} + \psi_{2,2}) + 2kc^2(w_{2,2} + \psi_{2,2} + w_{2,2}^2 + w_{2,2}\psi_{2,2}) + k\psi_{2,2}(w_{2,2} + \psi_{2,2}) + \psi_{1,2}k(w_{1,2} + \psi_{1,2}) + \psi_{2,2}kc^2(w_{2,2} + \psi_{2,2}) + v_{2,2}kc(w_{2,2} + \psi_{2,2}) \quad (e)$$

$$\kappa_{25} = 2kc \left[\psi_{2,2}(w_{2,2} + \psi_{2,2}) + \psi_{1,2}(w_{1,2} + \psi_{1,2}) + \psi_{2,2}^2(w_{2,2} + \psi_{2,2}) \right] \quad (f)$$

$$\kappa_{26} = (k^2/2) \left[w_{2,2}^2 + 2w_{2,2}\psi_{2,2} + \psi_{2,2}^2 + w_{1,2}^2 + 2w_{1,2}\psi_{1,2} + \psi_{1,2}^2 + c^2(w_{2,2}^2 + \psi_{2,2}^2 + 2w_{2,2}\psi_{2,2} + \psi_{2,2}^2) \right] \quad (g)$$

$$\kappa_{27} = k^2 c \left[(w_{2,2} + \psi_{2,2})^2 + (w_{1,2} + \psi_{1,2})^2 + c^2(w_{2,2} + \psi_{2,2})^2 \right] \quad (h)$$

$$\varepsilon_6 = \varepsilon_6^0 + \zeta^p \kappa_{6p}. \quad ()$$

$$\varepsilon_6^0 = u_{,2} + v_{,1} + u_{,1}u_{,2} + v_{,1}v_{,2} + w_{,1}w_{,2} + c(vw_{,1} - v_{,1}w)$$

$$\begin{aligned} \kappa_{61} = & c(u_{,2} - v_{,1}) + \psi_{1,2} + \psi_{2,1} + u_{,1}\psi_{1,2} + \psi_{1,1}u_{,2} \\ & c(u_{,1}u_{,2} - v_{,1}v_{,2} + w_{,1}w_{,2} - w\psi_{2,1} + w_{,1}\psi_2) + v_{,1}\psi_{2,2} \\ & + v_{,2}\psi_{2,1} \end{aligned} \quad (b)$$

$$\begin{aligned} \kappa_{62} = & c(\psi_{1,2} + u_{,1}\psi_{1,2} + u_{,2}\psi_{1,1} - cw\psi_{2,1} + cw_{,1}\psi_2) \\ & + \psi_{1,1}\psi_{1,2} + \psi_{2,1}\psi_{2,2} \end{aligned} \quad (c)$$

$$\begin{aligned} \kappa_{63} = & 2kw_{,12} + k\psi_{1,2} + k\psi_{2,1} + ku_{,2}(w_{,11} + \psi_{1,1}) \\ & + ku_{,1}(w_{,12} + \psi_{1,2}) + kv_{,1}(w_{,22} + \psi_{2,2}) \\ & + kcw_{,1}(w_{,2} + \psi_2) - kcw(w_{,12} + \psi_{2,1}) \\ & + c(\psi_{1,1}\psi_{1,2} + \psi_{2,1}\psi_{2,2}) + kv_{,2}(w_{,12} + \psi_{2,1}) \end{aligned} \quad (d)$$

$$\begin{aligned} \kappa_{64} = & kc(w_{,12} + \psi_{1,2}) + kcu_{,2}(w_{,11} + \psi_{1,1}) \\ & + \psi_{2,1}(w_{,22} + \psi_{2,2}) - kc^2(ww_{,12} + w\psi_{2,1} - w_{,1}w_{,2} \\ & - w_{,1}\psi_2) + k(\psi_{1,1}w_{,12} + 2\psi_{1,1}\psi_{1,2} + \psi_{1,2}w_{,11}) \\ & + \psi_{2,2}(w_{,12} + \psi_{2,1}) + kcu_{,1}(w_{,12} + \psi_{1,2}) \end{aligned} \quad (e)$$

$$\begin{aligned} \kappa_{65} = & kc(\psi_{1,1}w_{,12} + \psi_{1,2}w_{,11} + \psi_{2,1}w_{,22} + \psi_{2,2}w_{,12} \\ & + 2\psi_{1,1}\psi_{1,2} + 2\psi_{2,1}\psi_{2,2}) \end{aligned} \quad (f)$$

$$\kappa_{66} = k^2 \left[(w_{,11} + \psi_{1,1})(w_{,12} + \psi_{1,2}) + (w_{,12} + \psi_{2,1})(w_{,22} + \psi_{2,2}) \right]$$

$$\kappa_{67} = k^2 c \left[(w_{,11} + \psi_{1,1})(w_{,12} + \psi_{1,2}) + (w_{,12} + \psi_{2,1})(w_{,22} + \psi_{2,2}) \right]$$

$$\varepsilon_4 = \varepsilon_4^0 + \zeta^2 \kappa_{42}, \quad \varepsilon_4^0 = w_{,2}/\alpha_2 + \psi_2 \cdot \kappa_{42} - 3k\varepsilon_4^0 \quad (A5)$$

$$\varepsilon_5 = \varepsilon_5^0 + \zeta^2 \kappa_{52}, \quad \varepsilon_5^0 = w_{,1}/\alpha_1 + \psi_1 \cdot \kappa_{52} - 3k\varepsilon_5^0 \quad (A6)$$

$$U_1 = \frac{1}{2} \int_{\Omega} (u_1 + u_2 + u_3) d\Omega \quad (A7)$$

$$u_1 = \int_h \mathbf{x}^0 T Q \mathbf{x}^0 d\zeta = \int_h \varepsilon_j^0 \varepsilon_i^0 \bar{Q}_{ij} d\zeta$$

$$= \varepsilon_j^0 \varepsilon_i^0 A_{ij} \quad (a)$$

$$u_2 = \int_h 2\mathbf{x}^0 T Q \mathbf{x} d\zeta = \int_h 2\varepsilon_j^0 \bar{Q}_{ij} \kappa_{ip} \zeta^p d\zeta$$

$$= 2\varepsilon_j^0 (\kappa_{i1} B_{ij} + \kappa_{i2} D_{ij} + \kappa_{i3} E_{ij} + \kappa_{i4} F_{ij} +$$

$$\kappa_{i5} G_{ij} + \kappa_{i6} H_{ij} + \kappa_{i7} I_{ij}) \quad (b)$$

$$u_3 = \int_h \mathcal{Z}^T (\mathcal{K}^T Q \mathcal{K}) \mathcal{Z} d\zeta = \int_h \kappa_{jp} \kappa_{ir} \bar{Q}_{ij} \zeta^{p+r} d\zeta$$

$$= \kappa_{j1} \kappa_{i1} D_{ij} + 2 \kappa_{j1} \kappa_{i2} E_{ij} + (2 \kappa_{j1} \kappa_{i3} + \kappa_{j2} \kappa_{i2}) F_{ij}$$

$$+ 2(\kappa_{j1} \kappa_{i4} + \kappa_{j2} \kappa_{i3}) G_{ij} + (2 \kappa_{j1} \kappa_{i5} + 2 \kappa_{j2} \kappa_{i4}) H_{ij}$$

$$+ 2(\kappa_{j1} \kappa_{i6} + \kappa_{j2} \kappa_{i5} + \kappa_{j3} \kappa_{i4}) I_{ij} + (2 \kappa_{j1} \kappa_{i7} +$$

$$2 \kappa_{j2} \kappa_{i6} + 2 \kappa_{j3} \kappa_{i5} + \kappa_{j4} \kappa_{i4}) J_{ij} +$$

$$2(\kappa_{j2} \kappa_{i7} + \kappa_{j3} \kappa_{i6} + \kappa_{j4} \kappa_{i5}) K_{ij} + (2 \kappa_{j3} \kappa_{i7} +$$

$$2 \kappa_{j4} \kappa_{i6} + \kappa_{j5} \kappa_{i5}) L_{ij} + 2(\kappa_{j4} \kappa_{i7} + \kappa_{j5} \kappa_{i6}) P_{ij}$$

$$+ (2 \kappa_{j5} \kappa_{i7} + \kappa_{j6} \kappa_{i6}) R_{ij} + 2 \kappa_{j6} \kappa_{i7} S_{ij} + \kappa_{j7} \kappa_{i7} T_{ij}$$

(c)

where $i, j = 1, 2, 6$ and $p, r = 1, 2, 3, 4, 5, 6, 7$

$$\begin{aligned} \tilde{K} = & A_{ij} {}_0L_{i0} L_j^T + 2B_{ij} {}_0L_{i1} L_j^T + D_{ij} (2{}_0L_{i2} L_j^T + {}_1L_{i1} L_j^T) \\ & + E_{ij} (2{}_0L_{i3} L_j^T + 2{}_1L_{i2} L_j^T) + F_{ij} (2{}_0L_{i4} L_j^T + 2{}_1L_{i3} L_j^T \\ & + 2{}_2L_{i2} L_j^T) + G_{ij} (2{}_1L_{i4} L_j^T + 2{}_2L_{i3} L_j^T) + H_{ij} (2{}_2L_{i4} L_j^T \\ & + {}_3L_{i3} L_j^T) + 2I_{ij3} L_{i4} L_j^T + J_{ij4} L_{i4} L_j^T \end{aligned}$$

(A8)

$$\begin{aligned}
\tilde{N}_i = & A_{ij} \underline{L_i d^T} H_j + B_{ij} (\underline{L_i d^T} H_j + L_i d^T H_j) + D_{ij} (\underline{L_i d^T} H_j \\
& + L_i d^T H_j + L_i d^T H_j) + E_{ij} (\underline{L_i d^T} H_j + L_i d^T H_j \\
& + L_i d^T H_j + L_i d^T H_j) + F_{ij} (\underline{L_i d^T} H_j + L_i d^T H_j \\
& + L_i d^T H_j + L_i d^T H_j) + G_{ij} (\underline{L_i d^T} H_j \\
& + L_i d^T H_j + L_i d^T H_j + L_i d^T H_j + L_i d^T H_j) \\
& + H_{ij} (\underline{L_i d^T} H_j + L_i d^T H_j + L_i d^T H_j + L_i d^T H_j \\
& + L_i d^T H_j) + I_{ij} (\underline{L_i d^T} H_j + L_i d^T H_j + L_i d^T H_j \\
& + L_i d^T H_j + L_i d^T H_j) + J_{ij} (\underline{L_i d^T} H_j + L_i d^T H_j \\
& + L_i d^T H_j + L_i d^T H_j) + K_{ij} (\underline{L_i d^T} H_j + L_i d^T H_j \\
& + L_i d^T H_j) + L_{ij} (\underline{L_i d^T} H_j + L_i d^T H_j) + P_{ij} L_i d^T H_j
\end{aligned}$$

(A9)

note: underlined term is referred to in Eqn (34).

$$\begin{aligned}
\tilde{M}_2 = & A_{ij} {}_0H_i dd^T {}_0H_j + B_{ij} {}_0H_i dd^T {}_1H_j + D_{ij} ({}_0H_i dd^T {}_2H_j \\
& + {}_1H_i dd^T {}_1H_j) + E_{ij} ({}_0H_i dd^T {}_3H_j + 2{}_1H_i dd^T {}_2H_j) + F_{ij} ({}_0H_i dd^T {}_4H_j \\
& + 2{}_1H_i dd^T {}_3H_j + 2{}_2H_i dd^T {}_2H_j) + G_{ij} ({}_0H_i dd^T {}_5H_j + 2{}_1H_i dd^T {}_4H_j \\
& + 2{}_2H_i dd^T {}_3H_j) + H_{ij} ({}_0H_i dd^T {}_6H_j + 2{}_1H_i dd^T {}_5H_j + 2{}_2H_i dd^T {}_4H_j \\
& + {}_3H_i dd^T {}_3H_j) + I_{ij} ({}_0H_i dd^T {}_7H_j + 2{}_1H_i dd^T {}_6H_j + 2{}_2H_i dd^T {}_5H_j \\
& + 2{}_3H_i dd^T {}_4H_j) + J_{ij} (2{}_1H_i dd^T {}_7H_j + 2{}_2H_i dd^T {}_6H_j + 2{}_3H_i dd^T {}_5H_j \\
& + {}_4H_i dd^T {}_4H_j) + K_{ij} (2{}_2H_i dd^T {}_7H_j + 2{}_3H_i dd^T {}_6H_j + 2{}_4H_i dd^T {}_5H_j) \\
& + L_{ij} (2{}_3H_i dd^T {}_7H_j + 2{}_4H_i dd^T {}_6H_j + {}_5H_i dd^T {}_5H_j) \\
& + P_{ij} (2{}_4H_i dd^T {}_7H_j + 2{}_5H_i dd^T {}_6H_j) + R_{ij} (2{}_5H_i dd^T {}_7H_j \\
& + {}_6H_i dd^T {}_6H_j) + S_{ij} 2{}_6H_i dd^T {}_7H_j + T_{ij} {}_7H_i dd^T {}_7H_j
\end{aligned}$$

(A10)

REPORT DOCUMENTATION PAGE

1a. REPORT SECURITY CLASSIFICATION Unclassified			1b. RESTRICTIVE MARKINGS		
2a. SECURITY CLASSIFICATION AUTHORITY			3. DISTRIBUTION/AVAILABILITY OF REPORT Approved for public release; distribution unlimited.		
2b. DECLASSIFICATION/DOWNGRADING SCHEDULE					
4. PERFORMING ORGANIZATION REPORT NUMBER(S)			5. MONITORING ORGANIZATION REPORT NUMBER(S)		
6a. NAME OF PERFORMING ORGANIZATION Department of Engineering Mech. Dean of Faculty		6b. OFFICE SYMBOL (If applicable) USAFA/DFEM		7a. NAME OF MONITORING ORGANIZATION	
6c. ADDRESS (City, State and ZIP Code)		7b. ADDRESS (City, State and ZIP Code)			
8a. NAME OF FUNDING/SPONSORING ORGANIZATION		8b. OFFICE SYMBOL (If applicable)		9. PROCUREMENT INSTRUMENT IDENTIFICATION NUMBER	
8c. ADDRESS (City, State and ZIP Code)		10. SOURCE OF FUNDING NOS.			
		PROGRAM ELEMENT NO.		PROJECT NO.	TASK NO.
					WORK UNIT NO.
11. TITLE (Include Security Classification) Two Dimensional Laminated Shell Theory Including Parabolic					
12. PERSONAL AUTHOR(S) Transverse Shear Capt Scott T. Dennis					
13a. TYPE OF REPORT Final		13b. TIME COVERED FROM _____ TO _____		14. DATE OF REPORT (Yr., Mo., Day)	
15. PAGE COUNT					
16. SUPPLEMENTARY NOTATION					
17. COSATI CODES			18. SUBJECT TERMS (Continue on reverse if necessary and identify by block number)		
FIELD	GROUP	SUB. GR.	Shell Transverse Shear		
11	04		Nonlinear Finite Element		
			Composite Laminated Shell		
19. ABSTRACT (Continue on reverse if necessary and identify by block number)					
<p>The Report presents an approach for a general laminated shell geometry describable by orthogonal curvilinear coordinates. The theory includes a through the thickness parabolic distribution of transverse shear stress. Additionally, a simplified approach that allows large displacements and rotations is incorporated. The theory is cast into a displacement based finite element formulation and then specialized to a cylindrical shell geometry. Linear results are compared to exact elasticity solutions of a laminated cylindrical shell in cylindrical bending. The approach predicts displacement and stress for the unidirectional cases very well even for the very thick laminates. Transverse stress for the cross ply cases are not as accurate since equilibrium at the ply interfaces is not enforced, a typical drawback of 2-D theories.</p>					
20. DISTRIBUTION/AVAILABILITY OF ABSTRACT UNCLASSIFIED/UNLIMITED <input checked="" type="checkbox"/> SAME AS RPT. <input type="checkbox"/> DTIC USERS <input type="checkbox"/>			21. ABSTRACT SECURITY CLASSIFICATION UNCLASSIFIED		
22a. NAME OF RESPONSIBLE INDIVIDUAL Capt Scott T. Dennis			22b. TELEPHONE NUMBER (Include Area Code) 719-472-2889		22c. OFFICE SYMBOL USAFA/DFEM